Neuroscience and Biobehavioral Reviews 126 (2021) 213–235

Contents lists available at ScienceDirect

Neuroscience and Biobehavioral Reviews

journal homepage: www.elsevier.com/locate/neubiorev

Review article

Rodent somatosensory thalamocortical circuitry: Neurons, synapses, and connectivity

Christian O'Reilly [a,b,c,*], Elisabetta Iavarone [c], Jane Yi [d], Sean L. Hill [c,e,f]

[a] Azrieli Centre for Autism Research, Montreal Neurological Institute, McGill University, Montreal, Canada
[b] Ronin Institute, Montclair, NJ, USA
[c] Blue Brain Project, École Polytechnique Fédérale de Lausanne, Geneva, Switzerland
[d] Brain Mind Institute, École Polytechnique Fédérale de Lausanne, Lausanne, Switzerland
[e] Department of Psychiatry, University of Toronto, Toronto, Canada
[f] Centre for Addiction and Mental Health, Toronto, Canada

ARTICLE INFO

Keywords:
Thalamocortical loop
Thalamus
Microcircuit
Modeling
Reticular nucleus
Somatosensory system
Ventral posteromedial nucleus
Ventral posterolateral nucleus
Posterior nucleus
Thalamic relay cells
Thalamic interneurons
Rodent

ABSTRACT

As our understanding of the thalamocortical system deepens, the questions we face become more complex. Their investigation requires the adoption of novel experimental approaches complemented with increasingly sophisticated computational modeling. In this review, we take stock of current data and knowledge about the circuitry of the somatosensory thalamocortical loop in rodents, discussing common principles across modalities and species whenever appropriate. We review the different levels of organization, including the cells, synapses, neuroanatomy, and network connectivity. We provide a complete overview of this system that should be accessible for newcomers to this field while nevertheless being comprehensive enough to serve as a reference for seasoned neuroscientists and computational modelers studying the thalamocortical system. We further highlight key gaps in data and knowledge that constitute pressing targets for future experimental work. Filling these gaps would provide invaluable information for systematically unveiling how this system supports behavioral and cognitive processes.

1. Introduction

The thalamocortical (TC) loop is known to play a central role in cerebral rhythmogenesis (Buzsaki, 2006; Fogerson and Huguenard, 2016; Steriade, 2006, 2000). As such, it supports many functions, such as sleep and wakefulness (McCormick and Bal, 1997; Steriade et al., 1993, 1991; Timofeev et al., 2012), and is involved in various diseases associated with dysfunction of rhythmic activity (Schulman et al., 2011), such as epilepsy (Brodovskaya and Kapur, 2019; Halász, 2013; Nowack and Theodoridis, 1991; Timofeev et al., 2012), autism (Iidaka et al., 2019; Linke et al., 2018; Nair et al., 2013; Woodward et al., 2017), and schizophrenia and bipolar disorder (Anticevic et al., 2014b, 2014a; Baran et al., 2019; Ferri et al., 2018; Klingner et al., 2014; Murray and Anticevic, 2017; Skåtun et al., 2018; Woodward et al., 2012).

Further, the thalamus plays an important role in an array of cognitive processes. Initially considered to be a simple relay station passing along information between the cortex and the peripheral nervous system, the thalamus is increasingly understood as an intricate looped system working in tight interaction with cortical networks. Such interactions were proposed early (Miller, 1996) based on spreading depression experiments (Aquino-Cias et al., 1966; Bureš et al., 1965). Since then, optogenetic experiments demonstrated how continuous thalamic input is necessary for sustaining cortical activity (Reinhold et al., 2015) and how it supports behavioral tasks by enhancing functional cortical connectivity (Schmitt et al., 2017). In turn, cortical inputs shape thalamic activity through an extensive network of corticothalamic (CT) projections, outnumbering their thalamocortical (TC) counterpart by approximately an order of magnitude (Deschênes et al., 1998; Sherman and Koch, 1986). Through these projections, the cortex can, for example, sharpen the thalamic receptive fields to selectively enhance TC transmission of sensory information (Briggs and Usrey, 2008). Further, by modulating the level of hyperpolarization in TC cells, CT afferents can switch the mode of operation of these neurons between event detection (burst firing) and perception (tonic firing) (Ahissar and Oram,

* Corresponding author at: McGill University, 3775 Rue University, Room C18, Duff Medical Building, Montréal, Québec, H3A 2B4, Canada.
E-mail addresses: christian.oreilly@mcgill.ca (C. O'Reilly), sean.hill@epfl.ch (S.L. Hill).

https://doi.org/10.1016/j.neubiorev.2021.03.015
Received 1 July 2020; Received in revised form 15 February 2021; Accepted 14 March 2021
Available online 22 March 2021

2015). They can similarly leverage thalamic reticular cells to control sensory selection (Ahrens et al., 2015; Wimmer et al., 2015).

The thalamus has also been shown to preprocess raw peripheral inputs by encoding abstract functions. For example, this was demonstrated in the lateral geniculate nucleus (LGN) for center-surround inhibition, direction and orientation selectivity, and contrast evaluation in a visual scene (Piscopo et al., 2013). Similarly, cells from higher-order thalamic nuclei (HO) have been shown to encode stimulus-reward relationships by modulating their activity according to the detection of rewarded stimulus, the expected delay before reward, and the value of a reward (Komura et al., 2001). More generally, the thalamus has been proposed to play a central role in shaping mental representation (Wolff and Vann, 2019). This dual role as encoding mental representation and filtering input stimuli is supported by the convergence of ascending and descending afferents on thalamic targets. This convergence uniquely positions the thalamus for integrating bottom-up and top-down information streams and therefore for binding cognitive predictions with sensory input, as proposed by the predictive-coding theory (Groh et al., 2014). All these properties of the thalamus makes it a key component in a large number of cognitive domains (Saalmann and Kastner, 2015) such as learning (Bradfield et al., 2013), memory (Funahashi, 2013; Jankowski et al., 2013), language (Klostermann, 2013), attention (Kinomura et al., 1996), motor control (Prevosto and Sommer, 2013), and multisensory processing (Cappe et al., 2009).

In the last decade, large-scale *in silico* simulations have been developed with an ever-increasing level of biophysical details which allow us to better understand such complex systems. Simulation neuroscience has also proven to be invaluable for guiding or corroborating experimental investigations. Recent studies in this area have demonstrated how small volumes of brain tissue can be simulated using morphologically and biophysically detailed neuron models (Markram et al., 2015). Less detailed frameworks have also been used to perform large-scale simulations at the microscopic scale (i.e., the scale of the neuron) (Ananthanarayanan et al., 2009; Hill and Tononi, 2005; Izhikevich and Edelman, 2008; Schumann et al., 2017). Alternatively, other approaches have focused on the mesoscopic scale (i.e., the scale of a cortical column) using, for example, the neural field approach (Sanz Leon et al., 2013). These simulation frameworks provide platforms to integrate available knowledge and push forward our understanding of cross-scale, cross-species, and cross-modalities mechanisms underlying cognition and behavior.

As opposed to the cortical microcircuitry which has been modeled in fine detail, the TC circuitry has received relatively little attention. As we better appreciate the interdependencies between thalamic and cortical networks, the details of these interactions increase in significance. The rising awareness of the crucial role played by the TC loop in cerebral rhythmogenesis, in diseases associated with TC dysrhythmia, and in various cognitive processes motivates the comprehensive synthesis of current knowledge on thalamic microcircuitry proposed herein. In the following sections, we describe the TC system related to somatosensation, review the biophysics of its neurons and their synapses, the neuroanatomy of the related nuclei, its afferent and efferents, as well as its internal connectivity. We conclude by highlighting knowledge gaps that need to be addressed to allow computational neuroscientists to build accurate predictive models. This review focuses on the rodent somatosensory system but we also mention data from other species or thalamic regions whenever available and relevant.

2. Overview of the somatosensory TC loop

The thalamus is divided into two structures, the dorsal thalamus (also referred to simply as the thalamus) and the ventral thalamus (also known as the subthalamus or prethalamus) (Puelles et al., 2012). In the somatosensory system, the ventrobasal complex of the dorsal thalamus (VB) is comprised of two first-order nuclei (FO) responsible for relaying somatosensory signals: the ventral posteromedial nucleus (VPM) for the face and neck area and the ventral posterolateral nucleus (VPL) for the rest of the body. These nuclei receive their peripheral inputs through various pathways (i.e., the lemniscal, extralemniscal, and paralemniscal pathways; see Section 6.1). Other thalamic nuclei such as the nucleus submedius and the ventromedial nucleus also receive somatic input, probably respectively for nociception and sensorimotor integration (Ebner and Kaas, 2015), but will not be discussed here because of their secondary role with respect to somatosensation.

The rodent VB is mainly composed of excitatory TC cells that target the primary somatosensory cortex (S1). It primarily innervates the layers 4 (L4), but also to some extent, L2-3 and L5b-6 (Clasca et al., 2012; Meyer et al., 2010; see also Fig. 1; cortical efferents and laminar specificity are further discussed in Section 3.1.2). Additionally, it sends collaterals to the inhibitory reticular nucleus of the ventral thalamus (Rt). Although TC signals are amplified and further processed within a rather complex cortical microcircuitry (Markram et al., 2015), they are also fed back directly to the thalamus through monosynaptic pathways (Briggs and Usrey, 2007).

In general, cortical L5 and L6 pyramidal cells close the TC loop by projecting to their initial FO (i.e., VPM or VPL) as well as the associated HO, namely, for the somatosensory system, the medial sectors of the posterior nucleus (POm) (Ohno et al., 2012). These projections also send collaterals to Rt, which in turn generates inhibitory postsynaptic potentials (IPSP) in the same nuclei (i.e., VPL, VPM, POm). We should not oversimplify the effect of this parallel inhibitory pathway since the interplay of monosynaptic CT excitation and disynaptic cortico-reticulo-thalamic inhibition results in complex time-frequency properties. For example, at low frequency, the net effect of CT projections is briefly excitatory before becoming dominated by inhibition. However, at high frequency, it remains excitatory because of short-term facilitation of the CT synapses and short-term depression of Rt synapses

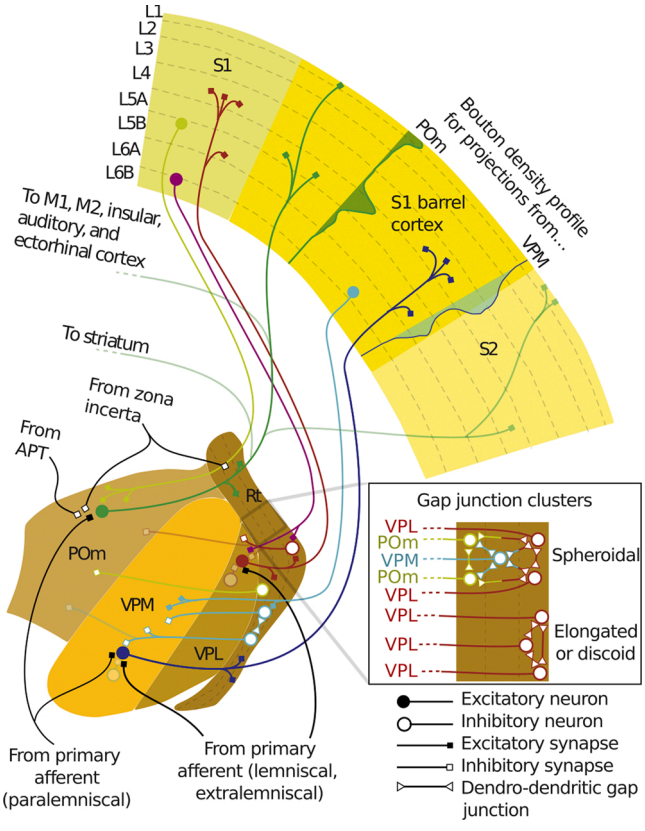

Fig. 1. Schema displaying the key features and primary pathways for the somatosensory TC loop in rodents. Bouton density profiles for VPM and POm projections are taken from (Meyer et al., 2010).

(Crandall et al., 2015; reviewed in Section 5.2).

On top of the afferents already discussed, POm also receives inhibition from extrareticular sources including the zona incerta (ZI) and the anterior pretectal nucleus (APT) (Bartho et al., 2002; Groh et al., 2014; reviewed in Section 6.3) and excitation from the paralemniscal pathway (Pierret et al., 2000; reviewed in Section 6.1).

In our schematic summary of the key features of the somatosensory TC system in rodents (Fig. 1), we separated the Rt into three tiers according to their projection targets (Lee et al., 2014; Pinault et al., 1995a). The specificity of tier targets by TC collaterals is yet unknown (Lee et al., 2014). About 90 % of TC-Rt connections are expected to form open-loop connections (reviewed in Section 5.4), probably to provide lateral inhibition. There is some disagreement on the presence of interneurons in VB, with proportions reported being between 0% and 4% (reviewed in Section 4.3). Clusters of gap junctions in the Rt (reviewed in Section 5.3) are shown as per Lee et al. (2014).

Projections from the anterior part of POm target preferentially L5, whereas those from the posterior part tend to further project to L1 with sparser and wider axonal arborization (Ohno et al., 2012). FO and HO TC projections tend to innervate complementary cortical lamina (Clasca et al., 2012; Meyer et al., 2010). Similar to TC cells in VB, projections from POm do not send intra-nucleus collaterals but send collaterals to Rt on their way to the cortex (Ohno et al., 2012). Most of them also send collaterals to the striatum – particularly for cells from the posterior part of POm – and also form arborization in other cortical regions, including secondary somatosensory (S2), primary and secondary motor, insular, auditory, and ectorhinal cortex (Ohno et al., 2012). Individual POm neurons send axons simultaneously to both S1 and S2 in a minority of cases (Ohno et al., 2012; Spreafico et al., 1987).

3. Thalamic neurons: their types and properties

A deep understanding of the inner workings of the TC loop is only possible with a thorough knowledge of the properties of its neurons, i.e., their morphologies, their electrophysiological behavior, their ion channels, and their synapses. Furthermore, establishing cell types across these different dimensions is fundamental for dissecting and reproducing this system *in silico*, an identification often facilitated by knowing the different protein markers expressed by these cells. These different aspects are reviewed in this section for the neurons of the VB (TC cells and interneurons) and the Rt (Rt cells). In rodents, FO contain relatively few interneurons, except for the LGN. Thus, most of the observations reported here were made on LGN interneurons, the knowledge on VB interneurons being much more scarce.

3.1. Morphological properties

3.1.1. Somata and dendrites

Early Golgi impregnation studies show that TC cells in the VPL have two to seven primary dendrites and predominantly fusiform somata in the coronal or horizontal planes, depending on their location in the VPL (McAllister and Wells, 1981). The discoid appearance of these neurons (e.g., see Fig. 2) follows the laminar organization of the VPL consisting in concentric circles centered around the VPM and running parallel to the Rt (McAllister and Wells, 1981).

An early study relying on visual inspection reported three variations of VB TC cells morphologies depending on whether their dendrites radiate in all directions (radiate) or along the rostrocaudal direction with (biconcave-radiate) or without (biconcave) a prominent group of dendrites radiating medially (McAllister and Wells, 1981). According to this study, the majority of VPL neurons would be biconcave, while VPM neurons would have more radiate dendritic fields, with larger and rounder somata (McAllister and Wells, 1981). However, subsequent studies reported no substantial evidence of subclasses of VB TC cells according to their somato-dendritic morphologies (Harris, 1986; Iavarone et al., 2019).

Fig. 2. Example of somato-dendritic morphologies of rat VB TC cells.

A more convincing subclassification of TC neurons has been demonstrated for the dorsal LGN (dLGN) of the mouse where three classes have been reported using quantitative assessment of their dendrites orientation: X-like (biconical, 22 %), Y-like (symmetrical, 49 %), or W-like (hemispheric, 29 %). All three types have large round somata and multipolar dendritic arbors, but the X-like type has significantly shorter dendrites and comparatively smaller somata (Krahe et al., 2011). They also have different spatial distribution within the dLGN: the majority of X-like cells are located near the borders with other nuclei (intergeniculate leaflet, ventral LGN), W-like cells are more often situated at the outer borders of the dLGN, while Y-like cells are more evenly distributed but with a larger prevalence within a central band running parallel to the optic tract. Similar classes have been described in the rat dLGN (Ling et al., 2012) with ~13 % of bipolar (biconical) cells aligned approximately parallel to the optic tract, ~55 % of radial (symmetrical) cells, and ~32 % of basket cells (similar to W-like type). Rats bipolar cells are located preferentially on the borders of the nucleus, similar to biconcave TC cells reported by (McAllister and Wells, 1981) in the VB.

Based on morphological features, membrane properties, response to stimuli, and differential immunofluorescence, mouse interneurons can be separated into two classes referred to as small and large soma types (9.3 ± 1.3 μm vs 11.7 ± 6.5 μm [mean ± sd], measured along their longest axis) (Leist et al., 2016). Interneuron somata are either spindle-shaped with primary dendrites branching from opposite poles or tripolar with three primary dendrites (Leist et al., 2016). They are about five times smaller than their TC counterparts, with mouse dLGN TC cells having an area of 1530 ± 170μm^2 (X-like; mean ± se), 2040 ± 460μm^2 (W-like), and 1710 ± 200μm^2 (Y-like) (Krahe et al., 2011), which correspond to 45−50 μm diameters for round somata. However, irrespective of their relatively small soma, mouse thalamic interneurons spread dendrites that arborize within broad areas of the dLGN (Morgan and Lichtman, 2020).

Dendrites in thalamic interneurons of rats produce varicose branches that end in beaded formations (Williams et al., 1996). Electron microscopy revealed synaptic vesicles in dendritic terminals which are thus said to be "axoniform" (Ralston, 1971). Inhibitory influences from both axonal and dendritic origins have also been shown pharmacologically (Cox and Sherman, 2000; Crandall and Cox, 2013). Dendritic terminals, also known as F2 terminals, contain more pleomorphic and sparsely distributed vesicles when compared with regular axonic (F1) terminals which have flattened and densely packed vesicles (Hamos et al., 1985).

In a nearly complete electron microscopy reconstruction, three thick dendrites were shown to emerge from the soma of a mouse thalamic interneuron. The dendrites progressed into thinner and circuitous neurites that were interlinked with swellings as previously described. These smaller dendrites ranged from short spike-like projections to longer (>50 μm) branched trees (Morgan and Lichtman, 2020).

Rt cells have oblong or discoid shapes and their dendrites are mostly parallel to the lateral border of the nucleus, i.e., along the plane formed by this sheet-shaped nucleus. Although the Rt can be divided along its thickness into functionally different tiers (e.g., see Rt projections in Fig. 1), most Rt dendrites cross these borders, allowing for information integration across different streams (Pinault, 2004). Existence of subtypes of Rt cells based on their morphology is debated (Pinault, 2004). Three types of Rt morphologies have been proposed based on the shape of their soma and the orientation of their dendritic fields : small fusiform (f-type), large fusiform (F-type), and round (R-type) (Spreafico et al., 1991, 1988). However, part of this variability may be due merely to constraints imposed on the dendritic field by the borders of the Rt (Pinault and Deschênes, 1998a). Further, some other authors report no subclass of Rt morphologies (Lubke, 1993; Ohara and Havton, 1996). Nevertheless, this classification seems to correlate with location along the anteroposterior axis (Vantomme et al., 2019) and with differences in electrical and chemical connectivity (Deleuze and Huguenard, 2006).

3.1.2. Axons morphology and cortical efferents

Depending on their cortical projections, TC cells can be separated into a core type, an intralaminar type, and a matrix type with either focal or multi-areal projections (Clasca et al., 2012). FO contain only core type cells (Clasca et al., 2012; Pape et al., 1994). These neurons tend to project most heavily to L4 (but see below for a more complete description of laminar projections) and to a limited region of primary sensory areas, sending coloraterals to Rt (Jones, 2007) but not within their own nucleus (Harris, 1987; Lee et al., 2010; Sawyer et al., 1994).

In VB, TC axons emerge from a prominent hillock and traverse the nucleus in a highly topographical manner, following an anterior-lateral direction, although neurons located more laterally in the nucleus sometimes follow a more unpredictable trajectory (Harris, 1987). Some arbors innervating the Rt have extensive branches contacting multiple Rt neurons, while others have a more limited extent (Harris, 1987).

With respect to the laminar specificity of TC projections, the classical understanding of the feedforward flow of information within the cortex considers that FO TC cells stimulate cortical neurons of the granular layer (L4). This activation is in turn relayed to the supragranular layer (L2/3) and then to the infragranular layer (L5/6) by local cortical projections (Gilbert and Wiesel, 1979). However, the actual pattern of innervation suggests many alternative routes within the cortical column (Feldmeyer, 2012). Aside from the many alternative pathways offered by the intricate intra-cortical connectivity (Feldmeyer, 2012), various pathways are already present at the level of the FO TC projections. Although these projections are most dense and potent in L4, they are by no means limited to this layer (Ji et al., 2016; Meyer et al., 2010). L1 inhibitory neurons and L2 to L6 excitatory cells and parvalbumin (PV) expressing inhibitory neurons have been shown to be innervated by these TC axons (Ji et al., 2016). Vasoactive intestinal polypeptide (VIP) and somatostatin (Sst) inhibitory neurons are for their part only targeted in L4 (Ji et al., 2016).

As opposed to FO, the POm, as a HO nucleus, contains matrix type cells, with more focal projections for TC cells in its lateral part and more multriareal projections for TC cells in its medial side (Clasca et al., 2012). These matrix projections tend to target lamina complementary to their FO core-type counterparts (Clasca et al., 2012; Meyer et al., 2010). Further, differences in laminar projections have also been reported along the antero-posterior axis of this nucleus, with its anterior part targeting more L5 and its posterior part targeting more L1 (Ohno et al., 2012). Such projections to L1 have been reported to be common for matrix axons and may allow substantial feedback interaction between cortical areas through these wide inter-areal thalamic projections (Rubio-Garrido et al., 2009). Further, this diversity of types of TC axons in HO nuclei may reflect the presence of parallel pathways, as suggested by differences in laminar and synaptic properties (i.e., ionotropic vs metabotropic) depending on their cortical targets. For example, projections from POm to cortical primary sensory regions are dominated by modulator characteristics whereas its projections to primary motor areas are more typical of drivers (Casas-Torremocha et al., 2019).

Reconstructed interneuron axons were shown to ramify locally within the LGN, with a small caliber, frequent *en passant* varicosities (Zhu and Lo, 1999a), and F1 terminals (Hamos et al., 1985). They resembled the thinner and circuitous dendrites that were located distally from the interneuron soma and possessed a relatively small arbor with only 5 terminal neurites in the single cell reconstruction of Morgan and Lichtman (2020). The small size of the interneuron axon is in agreement with previous light microscopy reconstructions (Zhu and Lo, 1999a) and indicates a limited functionality for these axons, as compared to these interneuron dendrites. The relative contributions of interneuron axons and dendrites is further explained in Sections 5.2.4 and 5.2.5.

In a series of experiments using juxtacellular recordings in rats (Pinault, 2004; Pinault et al., 1995b, 1995a; Pinault and Deschênes, 1998a), Rt axons were reported to project in a topographically precise manner (i.e., somatotopic for cells projecting to POm and VB), generally to single nuclei — with a few exceptions of cells projecting to corresponding FO and HO — and without making local collaterals within Rt. Most Rt axons branch locally in the thalamus and contact mainly distal dendrites of TC cells (Guillery and Harting, 2003; Pinault and Deschênes, 1998a).

3.2. Electrophysiological properties

3.2.1. Burst and tonic firing in TC and Rt cells

Rt and TC cells from different thalamic nuclei and species can fire bursts and tonic trains of action potentials (Jahnsen and Llinas, 1984). The former is a calcium-mediated low-threshold spike superimposed with high-frequency discharges of sodium spikes. Bursting in TC and Rt cells is elicited from hyperpolarized membrane potentials and contributes to the oscillations recorded in EEG during slow-wave sleep, like slow waves (< 1 Hz) (Steriade et al., 1993) and sleep spindles (7−14 Hz) (Steriade et al., 1987). The tonic spike trains consist of a low-frequency sequence of sodium spikes and is most common at depolarized membrane potential during alert states in vivo (Jones, 2002). These two firing modes are associated with different states of neuronal responsiveness, e.g., TC neurons respond only to low-frequency stimuli (<15 Hz) when bursting, but can relay inputs at frequencies as high as 100 Hz in tonic mode (McCormick and Feeser, 1990). Further, the tonic mode integrates linearly the inputs from TC afferents and therefore can reliably process sensory information, whereas burst firing acts in a nonlinear way and rather encodes an all-or-none relationship which can efficiently support event detection (Sherman, 2001; Ahissar and Oram, 2015). The possibility for external inputs to switch TC and Rt cells between these two states is a fundamental characteristic of the thalamus (Sherman, 2001). It can be leveraged to control functional properties across the whole TC loop, as shown for example by the suppression of cortical paired-pulse facilitation after switching TC cells from bursting to tonic mode using an optogenetic depolarization (Whitmire et al., 2017).

The switching between firing modes can be triggered by modulating the level of hyperpolarization of the TC cell, with sustained (~100 ms) depolarization inactivating the low-threshold (T-type) calcium current (I_T) necessary for bursting and consequently setting the cell in a tonic firing mode. Conversely, similarly sustained hyperpolarization de-inactivates these I_T-related ion channels and moves back the cell in bursting mode (Sherman, 2001). Processes associated with circadian rhythms are likely to contribute to the activation of this switching mechanism, as suggested by the association of bursting with

sleep-related rhythms such as spindles (Steriade et al., 1987; Lüthi, 2014) and slow waves (Steriade et al., 1993; Hughes et al., 2002). It is also further supported by the higher prevalence of bursting in sleep; burst-related action potentials during wakefulness has been reported to account for less than 1% of all action potentials, a proportion that goes up to 18 % during sleep (Weyand et al., 2001).

Even though TC and Rt cells share a similar bursting capability, the presence of small-conductance Ca^{2+}-activated SK-type K^{+} currents endows Rt cells with a natural tendency to generate repetitive bursts following a single stimulation (Cueni et al., 2008). Further, this property of Rt cells makes them more prone to generate oscillations like sleep spindles (Wimmer et al., 2012), as initially demonstrated in cats by spontaneous spindle generation in deafferented Rt (Steriade et al., 1987) but not in TC cells deafferented from the Rt nucleus (Steriade et al., 1985). Also, compared to TC cells, Rt cells have a more heterogeneous bursting behavior and can be subdivided into different firing types according to their bursting propensity, such as non-bursting, bursting, or atypically bursting (Clemente-Perez et al., 2017; Lee et al., 2007; see Fig. 3). The bursting characteristics can also be separated in terms of PV and Sst cell markers in the Rt: PV+ neurons have more sodium spikes within their calcium burst and an increased tendency to rebound, whereas Sst+ neurons have weak bursts and sometimes do not burst at all (Clemente-Perez et al., 2017). Protein markers are further discussed in Section 3.3.2.

Although characterized by an homogeneous bursting behavior across cells and nuclei (Bartlett and Smith, 1999), TC neurons display a more diverse repertoire of tonic firing responses. For example, VB TC cells of cats exhibit accelerating, accommodating, intermittent and accommodating, and burst-suppressed firing (Iavarone et al., 2019; Turner et al., 1997) as well as delayed firing (Huguenard and Prince, 1991). Spike-frequency adaptation during tonic firing was also shown in the visual thalamus for cats (Smith et al., 2001) and, to a lesser degree, for rats (Iavarone et al., 2019; Williams et al., 1996). Similarly, about 50 % of the neurons in the medial geniculate body (MGB) display noticeable adaptation (Bartlett and Smith, 1999). Such paired-pulse adaptation is responsible for the reported phase advance in the response of TC cell to slow sinusoidal current injections (Smith et al., 2001) and was associated with improved encoding of the spatiotemporal context of stimuli (Liu et al., 2017). Tonic firing also exhibits a particularly variable range of responses in HO TC cells (Li et al., 2003).

These different firing modes (tonic and burst) and levels of paired-pulse adaptation have been demonstrated to be reproducible in experimentally-constrained and biophysically-detailed TC cell models (Iavarone et al., 2019, see Fig. 4).

3.2.2. *Depolarizing sag*

A depolarizing "sag" in response to hyperpolarizing current injection has been observed in TC cells of different nuclei and species, such as in the ventral division of the MGB (vMGB) (Bartlett and Smith, 1999), in the dLGN neurons of rats and mice (Krahe et al., 2011; Williams et al., 1996), and in a fraction of the rat VB neurons (Pinault, 2003). This sag has been associated with the I_H current and more specifically with HCN4 channels, an isoform present in various dorsal thalamic nuclei including VB, but absent from the Rt (Zobeiri et al., 2019). This sag interacts with I_T currents and is therefore functionally relevant for bursting and thalamic burst-related rhymes such as slow waves and sleep spindles (Curró Dossi et al., 1992; Datunashvili et al., 2018; McCormick and Pape, 1990).

3.2.3. *NMDA spikes*

Synaptic input limited to single TC dendrites were shown to be sufficient to trigger NMDA spikes/plateaux in LGN TC cells of rats and mice (Augustinaite et al., 2014). Due to the electrotonic compactness of TC cells, even NMDA spikes generated on distal dendrites can reach the soma, providing a powerful control mechanism for CT cells targeting these sites. These spikes can trigger bursting in quiescent hyperpolarized TC cells or can inhibit subsequent bursting by preventing T-channels de-inactivation in cells that recently bursted (Augustinaite et al., 2014). When TC cells are in tonic mode, NMDA spikes tend not to cause action potentials but to increase the rate of successful transmission of incoming action potentials, potentially providing an efficient mechanism for cortical control of incoming stimuli by facilitating TC cell spiking. In L5 pyramidal cells, NMDA spikes have been reported to cause long-lasting depolarization in dendritic trees and constitute a cellular mechanism for the temporal binding of information and synaptic modification (Antic et al., 2010). It is currently unclear if they serve a similar role in the

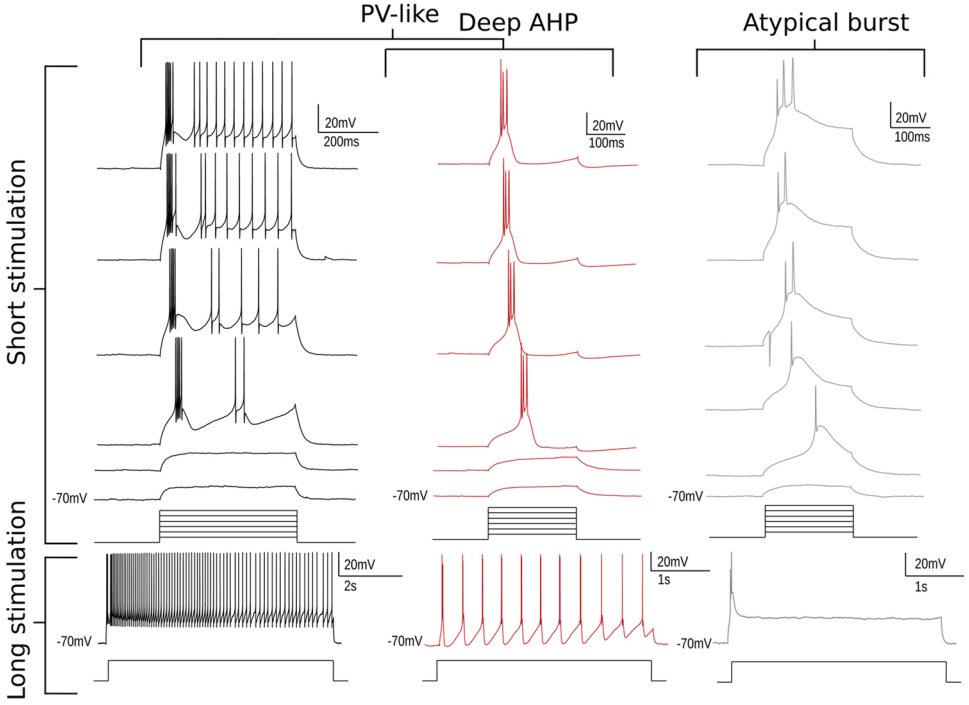

Fig. 3. Examples of PV-like burst, atypical burst, and non-bursting Rt neurons. Left three columns in P14-P18 rats, right column in P14-P18 mice (Yi et al., *in prep*).

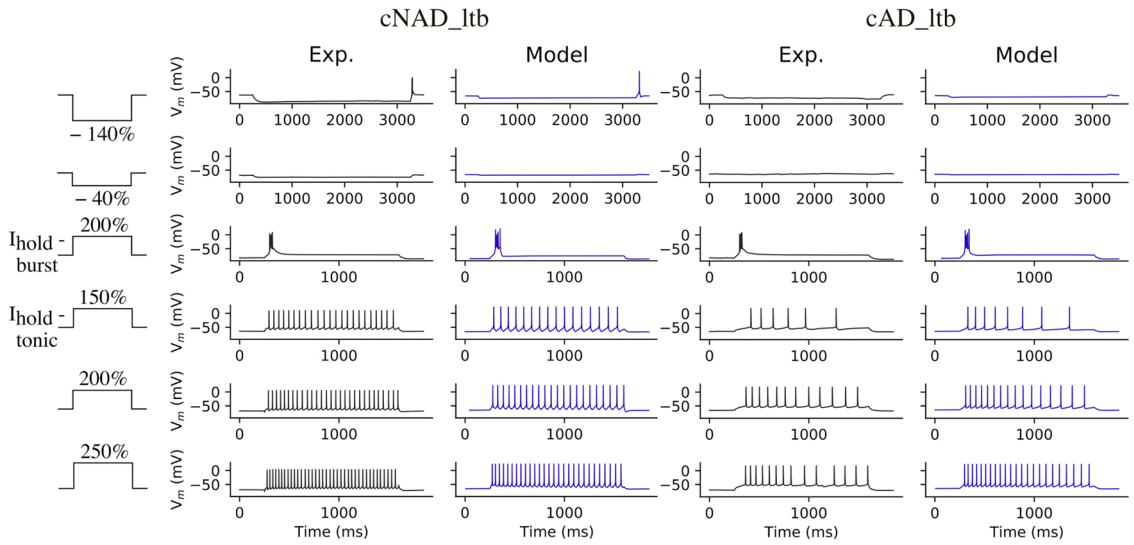

Fig. 4. Example of continuous adapting (cAD) and continuous non-adapting (cNAD) low threshold burst (ltb) for TC neurons of the VB in models and experiments. Exp: experiment. Adapted from Iavarone et al. (2019) with permission.

thalamus.

3.2.4. Interneurons

In interneurons, a depolarizing square current pulse evokes a train of action potentials, which sometimes exhibit a slight oscillatory bursting (Leist et al., 2016). An intrinsic subthreshold oscillation of the membrane potential at approximately 8 Hz has also been described (Williams et al., 1996). Rat interneurons have a moderately higher resting membrane potential compared to TC cells (interneurons: −52 mV; TC: −63 mV) (Williams et al., 1996). In mice, resting membrane potentials are slightly different for small versus large soma interneuron types (small: -62.4 mV; large: -64.8 mV). Also, small, but not large, interneurons exhibited rebound bursting after a hyperpolarizing pulse and had a pronounced voltage sag, which is indicative of a higher I_h density (Leist et al., 2016).

According to the prosomere developmental model, the caudal part of the forebrain can be divided in three transverse domains along the rostrocaudal axis (p1-p3), which later forms the pretectum (p1), the dorsal thalamus and the habenula (p2), and the ventral thalamus (p3) (Nakagawa, 2019). Interestingly, recent investigations suggest that thalamic interneurons have an extra-thalamic origin and that they are mainly seeded from the tecal population (Jager et al., 2016). More precisely, all FO interneurons and 80 % of HO interneurons develop from the embryonic tectum, with the remaining 20 % deriving from the forebrain (Jager et al., 2021, 2016). This common origin of FO interneurons is indicative of their similarities across sensory modalities and echoes the consistency observed with respect to the origin, morphologies, and electrical properties of TC cells across modalities. It is further worth emphasizing that thalamic interneurons and Rt cells have a different origin, and hence, these two types of inhibitory cells may show significant functional differences (Jager et al., 2016).

3.3. Molecular properties

3.3.1. Ion channels

Firing modes of TC and Rt neurons critically depend on the subtypes of ion channels they express. Due to its role in burst firing, I_T currents are one of the most studied ionic currents in the thalamus and depends on the $Ca_V3.1$ isoforms in TC neurons (Talley et al., 1999) and the $Ca_V3.2$ (30 %) and $Ca_V3.3$ (70 %) isoforms in Rt cells (Astori et al., 2011). In Rt cells, calcium imaging indicates that I_T density increases from proximal to distal dendrites, reaching a peak at around 100 μm from the soma (Crandall et al., 2010). In TC neurons, the $Ca_V3.1$ channels are distributed in somata and dendrites, with early electrophysiological studies suggesting a higher density in stem dendrites compared to the soma (Williams and Stuart, 2000) and subsequent studies demonstrating their presence in intermediate and distal dendrites (Errington et al., 2010). Because TC cells are electrotonically compact in the somatofugal direction, $Ca_V3.1$ channels generate "global spikes" by triggering low-threshold bursts simultaneously across the whole dendritic tree (Connelly et al., 2015). The presence of $Ca_V3.1$ channels on distal dendritic sites has been suggested to support the amplification of CT inputs targeting these sites (Errington et al., 2010), while knocking down their corresponding gene in mice has been associated with disturbances of delta waves and sleep (Astori and Lüthi, 2013).

Hyperpolarization-activated cationic current (I_H) also contributes to burst firing in TC and Rt neurons. This current depends on HCN ion channels, which all four known isoforms are expressed in varying degrees across the thalamus of the rat. In particular, the neuropil of VB shows moderate to intense immunoreactivity for HCN1, HCN2, and HCN4 (Notomi and Shigemoto, 2004), with levels increasing significantly during development (i.e., approximately a 6-fold increase between P3 and P106) (Kanyshkova et al., 2009). The Rt contains HCN4-immunoreactive cell bodies and its neuropil is highly (HCN2) to moderately (HCN3, HCN4) immunoreactive for HCN isoforms (Notomi and Shigemoto, 2004). In mice, HCN2 and HCN4 are the major types expressed in VB and Rt (Abbas et al., 2006; Leist et al., 2016), with Rt cells being about 10 times more immunoreactive for HCN2 but equally immunoreactive for HCN4 when compared to TC cells (Abbas et al., 2006). Differential distribution of HCN2 channels within TC and Rt morphologies is also likely to be associated with significant differences in I_H properties in these two cell types. Further, given that I_H kinetics varies across HCN isoforms, changes in their relative proportions may be linked with functional differences (Santoro et al., 2000).

In rats, L-type high-voltage activated Ca^{2+} currents have also been recorded in dLGN TC cells, interneurons, and Rt neurons. Highest densities were found at the base of TC dendrites, in more central somatic regions for Rt cells, and uniformly distributed across the soma for interneurons (Budde et al., 1998). These currents are likely to work in close interaction with T-channels to control the bursting activity and the homeostasis of calcium concentration (Budde et al., 1998; Zhang et al., 2002).

Calcium influx in TC and Rt neurons contributes to the activation of Ca^{2+}-activated potassium currents of the SK (small conductance) and BK (big conductance) types. In rats, the SK2 ($K_{Ca}2.2$) type dominates in Rt and TC cells (Gymnopoulos et al., 2014). These channels are responsible

for repetitive bursting in Rt cells (Astori et al., 2013; Cueni et al., 2008). In the dLGN TC neurons of rats, the activation of BK channels was shown to decrease the number of action potentials per burst and increase the adaptation during tonic firing (Ehling et al., 2013). Specific antibodies against BK channels intensely stains all dorsal thalamic nuclei as well as the Rt in mice (Sausbier et al., 2006).

In mice VB, TC neurons were also found to have M-type potassium currents ($K_V7.2$ and $K_V7.3$ subunits) which helps hyperpolarizing their membrane and deinactivating I_T (Cerina et al., 2015) as well as A-type K^+ currents (I_A; $K_V4.1$-K4.3 subunits) which act as a functional antagonist of I_T and modulate the kinetics and amplitude of the low-threshold spike during burst firing (Kanyshkova et al., 2011).

Like LGN TC cells, interneurons have been shown to have I_T and I_A currents. However, the ranges of steady-state activation and inactivation of these two currents are highly overlapping (Pape et al., 1994). Thus, the I_A current causes a net membrane current counteracting the I_T-driven regenerative low-threshold Ca^{2+} response and results in a different firing pattern than the low-threshold burst displayed by TC and Rt cells (Pape et al., 1994).

Background K^+ channels (such as two-pore-domain, K_2p) TASK and TREK play a critical role in switching between activity states in TC neurons. These channels are also extensively modulated by neurotransmitters, such as muscarinic acetylcholine receptors (Bista et al., 2015).

A persistent sodium current is also active in soma and dendrites of TC neurons from rats dLGN, both during tonic and burst firing (Parri and Crunelli, 1998).

3.3.2. Protein markers

Molecular markers such as calcium-binding proteins (CBPs) and neuropeptides can be identified with conventional histological procedures and have been instrumental in differentiating cell types. In general, excitatory neurons express only a limited number of common markers and this is true for TC neurons as well. For example, some calcium-binding proteins, such as calretinin (CR), have been detected only in HO (Lu et al., 2009). In rats, PV has been shown to be virtually absent from the dorsal thalamus, while calbindin (CB) was absent from VB TC cells but was expressed in about two-thirds of POm TC cells (Rubio--Garrido et al., 2007). A differential distribution of PV and calbindin (CB) also distinguishes FO and HO auditory nuclei in mice, with PV densely and CB weakly expressed in vMGB neuropil (FO) and an inverted pattern in the auditory HO. The identity of the cells contributing to this PV immunoreactivity is, however, unclear since it can be associated with PV+ fibers coming from different origins, including Rt axons, ascending auditory fibers, and descending projections from the auditory cortex (Cruikshank et al., 2001).

PV antibody labeling also differentiate VB afferents: projections from Rt neurons are GABA+ and PV+, dendritic terminals from local inhibitory interneurons are GABA+ and PV-, and ascending terminals are GABA- and PV+ (De Biasi et al., 1994). Faintly labeled CB+ cells were found in the caudal part of the VPL, while the VPM is almost devoid of CB+ cells. PV+ and CR+ fibers can also be found in the VPL (Arai et al., 1994).

The results of immunoreactivity for CBPs are more complicated in the dLGN (Arai et al., 1994), with CR labeling numerous fibers but few cell bodies (Winsky et al., 1992). In some studies (Meuth et al., 2006; Okoyama and Moriizumi, 2001), PV was suggested to be a marker of TC neurons at least in the magnocellular part of the vLGN. However, other studies found TC cells to be PV- (Lintas et al., 2013; Luth et al., 1993). Confounders may partially explain these conflicting results. For example, dorsal thalamus nuclei can show PV immunoreactivity due to incoming fibers without expressing it locally in TC cells (Cruikshank et al., 2001; Luth et al., 1993) and PV mRNA but not PV proteins may be found in rat TC cells (Sieg et al., 1998). Further, although TC cells are PV- in rodents (Lintas et al., 2013; Luth et al., 1993) these cells — or at least a proportion of these cells — seem to be PV+ in monkeys (Jones and Hendry, 1989; Rausell and Jones, 1991; Rausell et al., 1992). One of these studies (Rausell et al., 1992) differentiated regions of the VPL that were rich in cytochrome oxidase (CO) from regions that were CO-weak. They reported TC cells to be smaller, PV-, and CB+ in CO-weak compartments, whereas PV+ and CB+ cells were found in CO-rich compartments. These differences in protein markers were further associated with different pathways as shown by cells from these two types of compartments having differential laminar projections to the cortex. The spinothalamic pathway has also been shown to be concentrated in CO-weak compartments. Furthermore, such pathway segregation has been recently demonstrated in the mouse whisker system (El-Boustani et al., 2020; more on the different pathways associated with the somatosensory system in Section 6).

Similarly to other inhibitory neurons in the brain, different types of CBPs and neuropeptides are expressed in Rt cells. This property could prove useful for parcellating this nucleus which is already known to be heterogeneous in terms of functional topographic maps and thalamic and cortical connections (see Section 4.4; Mitrofanis and Guillery, 1993). In rats, PV is present in all Rt sectors, while CR and CB are mostly expressed in the ventromedial corner of the rostral portion of Rt (Arai et al., 1994; Winsky et al., 1992). In mice, Sst and PV can be found across the entire anterior-posterior axis of the Rt, with a different distribution of Sst+ neurons in the medial-lateral extent of the somatosensory sector (Clemente-Perez et al., 2017). Differences in the expression of these two proteins allows segregating two functionally distinct subpopulations of Rt neurons (Ahrens et al., 2015; Clemente-Perez et al., 2017). By acting through the Sst-5 receptors of Rt cells, Sst can inhibit the GABA release and the oscillatory activity of these cells (Clemente-Perez et al., 2017; Leresche et al., 2000; Sun et al., 2002). Similarly, the neuropeptide cholecystokinin (CCK) has been shown to affect the firing behavior of Rt neurons and the oscillatory state of the thalamic network by suppressing a K^+ conductance (Cox et al., 1997). Neuropeptide-Y (NPY) and its receptors are also present in Rt neurons, allowing these cells to auto-regulate Rt activity by releasing NPY in a recurrent manner (Sun et al., 2003).

4. Neuroanatomy and cell composition

4.1. Parcellation

A 3D volume parcellation of the brain is required in various applications, such as for atlasing cell types (Erö et al., 2018) and their connections (Fürth et al., 2018), for modeling the brain at a cellular resolution (Markram, 2006), or for comparing brain characteristics (e.g., volume of regions) between conditions (e.g., age, gender, diseases). Two-dimensional stereotaxic atlases have been made available to allow precise positioning in context of experimental surgical manipulations in mice (Paxinos and Franklin, 2013) and rats (Paxinos and Watson, 2014). Although these resources can be used to generate volumetric atlases (Majka et al., 2012), the process of stacking annotated 2D slices creates severe artifacts due to partial misalignment of slightly distorted slices. As an alternative, the Allen Mouse Brain Connectivity Atlas provides a finely parcellated atlas of over 800 brain structures specified within their Common Coordinate Framework (CCF) and based on a population average of over 1,200 mice (Oh et al., 2014). For the rat, the Waxholm Space Atlas of the Sprague Dawley Rat Brain has been built from ex-vivo magnetic resonance imaging (MRI) and diffusion tensor imaging and provides a reconstruction free from slicing artifacts (Papp et al., 2014). However, due to the lower resolution of MRI compared to optical microscopy, this atlas currently[1] contains a coarser parcellation of the brain with 118 major anatomical structures and no thalamic subregions.

Initiatives like the CCF have proven to be highly useful, but a finer

[1] As of May 26th 2020, using the version stored on the NeuroImaging Tools & Resources Collaboratory website (https://www.nitrc.org).

parcellation is still needed to support the development of increasingly detailed models. For example, quantitative resources for somatotopy are still direly needed. Such data have often been collected (e.g., for the barrels (Meyer et al., 2013); see Section 4.4) but have not necessarily been standardized and released as a shared resource. For the thalamus, aside from functional maps (e.g., for somatotopy, tonotopy, and retinotopy), better quantitative data on the division of the Rt (e.g., head, tail, and tiers) (Clemente-Perez et al., 2017; Lam and Sherman, 2011; Pinault and Deschênes, 1998a) would be invaluable for mapping connectivity. Similarly, most somatosensory thalamic nuclei could be subdivided in smaller subregions than what is typically available in atlases, i.e., PO can be divided into four sub-nuclei (Sumser et al., 2017), VPM can be divided in dorsomedial (VPMdm), ventrolateral (VPMvl), and parvocellular parts (VPMpc) (Haidarliu et al., 2008), and the VPL can be split in caudal (VPLc), middle (VPLm), and rostral (VPLr) regions (Francis et al., 2008).

4.2. Stereological studies

Cell distributions in the whole brain have been recently made available, mostly for mice due to the development of genetically modified strains. For example, an atlas reporting the position in space of every cell of a mouse brain has been created using CUBIC-X expansion microscopy and tissue clearing (Murakami et al., 2018). This resource is currently limited since the propidium iodide fluorescent agent used for labeling cannot distinguish glial cells from neurons, but the same technique can be combined with immunostaining or transgenic mouse lines to provide a more precise identification of cell types. Other resources mapping individual cell types (Erö et al., 2018) or counting cells expressing different CBPs (i.e., PV, Sst, and VIP) (Kim et al., 2017) across the mouse brain have also recently been made available. These new resources are a welcomed addition to stereological studies of the thalamus since the latter provide relatively scarce and very inconsistent information. Reported cell densities in the rodent thalamus (Diaz et al., 1999; Huusko and Pitkanen, 2014; Lifshitz et al., 2007; Luczynska et al., 2003; Meyer et al., 2013; Mooney and Miller, 2010, 2007; Parent and Descarries, 2008; Ramos et al., 1995; Ross et al., 1995; Yamada et al., 2001) span over two orders of magnitude and show a clear and sizable between-laboratory effect (see Fig. 5), plainly illustrating the low reliability of these estimates, a result similar to what has been observed all across the mouse brain (Keller et al., 2018).

4.3. Presence of interneurons

In rodent FO, the presence of interneurons differs significantly across modalities. In the visual system, the dLGN is composed of a sizable proportion of interneurons, although the exact numbers vary greatly between studies (see Table 1).

In contrast, interneurons are very sparsely distributed in non-visual FO. Early studies were even suggesting their absence from VB (de Biasi et al., 1986; McAllister and Wells, 1981; Ottersen and Storm-Mathisen, 1984), but more recent investigations reported proportions around 0.4–1.0 % (Arcelli et al., 1997; Harris and Hendrickson, 1987). A recent study reported significantly higher proportions (4.2 % in VPM; 3.7 % in VPL) using light microscopy immunocytochemistry with a GABA immunogold marker in 6–12 months old Wistar rats (Cavdar

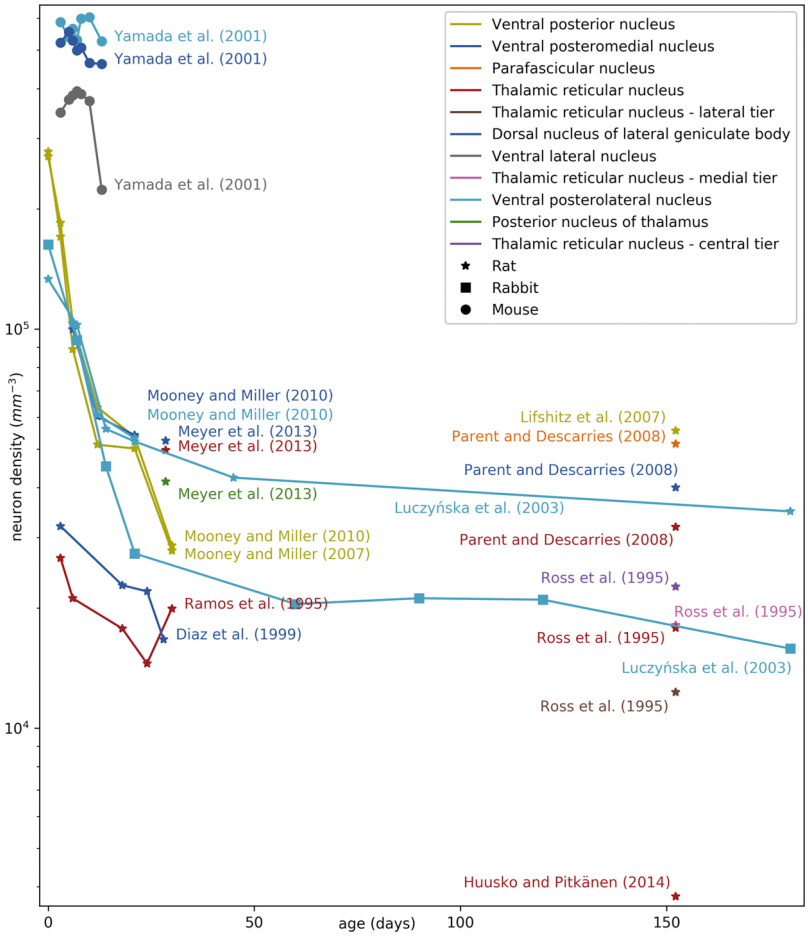

Fig. 5. Cell densities for different thalamic nuclei, in different rodent species, and at different ages. Data pooled from a systematically annotated corpus of literature on the rodent thalamus (O'Reilly et al., 2018, 2017).

Table 1
Reported percentages of interneurons in dLGN.

Percentage	Method	Species	Reference
5.8 %	GABA-immunopositive interneurons counted with optical fractionator	mice	(Evangelio et al., 2018)
8 %	Golgi staining and two-dimensional counting	mice	(Werner et al., 1984)
15–20 %	GABA immunostaining and thionin two-dimensional counting	various species	(Arcelli et al., 1997)
20–25 %	unlabeled cells after massive injection of HRP into areas 17 and 18	cats	(LeVay and Ferster, 1979)

et al., 2014). Low proportion of interneurons in VB is characteristic of rodents, this proportion being around 20–30 % in cats and primates (Arcelli et al., 1997; Penny et al., 1983; Spreafico et al., 1983).

This low prevalence is not sufficient to disregard any significant role since interneurons have been shown to serve important functions in regions with similarly low proportion, like in the striatum (Koós and Tepper, 1999). Further, interneuron connectivity has been ascribed some peculiar functional features such as triadic circuitry (Section 5.2.5; Sherman, 2004) and presynaptic dendrites (Cox and Beatty, 2017). Moreover, computational experiments suggest that they may serve essential roles such as transitioning between brain states (Bhattacharya et al., 2016).

4.4. Functional organization

The cellular composition and the neuronal projections have a very organized topology across the different types of thalamic nucleus (i.e., Rt, FO, and HO) and across the sensory modalities. For the somatosensory system, it is most clearly evidenced in VPM by the presence of whisker barreloids, the thalamic counterpart of cortical barrels (Hoogland et al., 1987; Sugitani et al., 1990; Van Der Loos, 1976). Cellular density has been shown to vary substantially across barreloids, increasing by about 50 % when going from E1 to A4 barreloids (Fig. 6; Meyer et al., 2013). This regional specificity demonstrates not only the importance of modeling differences between septal and barreloid regions but also across barreloids. In general, the whole VB has a somatotopic arrangement (Emmers, 1965; Saporta and Kruger, 1977; Waite, 1973), with a primary somatotopic map containing unilateral representations and a secondary with bilateral projections (Emmers, 1965).

POm has also been shown to be somatotopic (Fabri and Burton, 1991; Nothias et al., 1988; Ohno et al., 2012), with cortical driver projections from L5b innervating four distinctly oriented somatotopic maps in different subdivisions of this nucleus (Sumser et al., 2017). Early investigations have shown a clearer arrangement in VB than in Rt and POm (Hoogland et al., 1987). However, a more recent study reported VB and POm somatotopic maps to be equally well defined (Alloway et al., 2003), suggesting that the precision of such spatial mapping might be conserved along the pathways from FO to HO.

For the auditory system, the MGB can be divided into ventral/lemniscal (vMGB) and dorsal/extralemniscal (dMGB) parts. Whereas tonotopic organization has been shown in the former, it is absent in the latter (Bartlett and Smith, 1999). More precisely, four, possibly five, distinct tonotopic maps have been identified in the vMGB, with projections to different subregions of the auditory and the insular cortex. See Tsukano et al. (2017) for a review.

For the visual system, the dLGN has long been known to be retinotopic (Reese, 1988; Reese and Jeffery, 1983; Roth et al., 2016). The dLGN is further structured, with regions specific for ipsilateral versus contralateral inputs and different TC cell types in different subregions. Kerschensteiner and Guido (2017) recently reviewed the organizational principles within this nucleus.

Regarding the Rt, it has also been shown to have a topographic organization along its plane (sectors) and across its thickness (tiers) (Fig. 7A; Crabtree, 1999; Crabtree et al., 1998; Jones, 1975; Lam and Sherman, 2005; Pinault, 2004; Shosaku et al., 1984). The posterior part of this nucleus is separated in a dorsal region responding to visual stimuli in a retinotopic way (Hale et al., 1982) and a ventral region responding to auditory stimuli. A somatotopic representation of the different whisker receptive fields and the other body parts is found anterior to the visual and auditory sectors (Fig. 7B; Shosaku et al., 1984). The most ventral part of Rt is associated with taste (Hayama et al., 1994) and the region immediately dorsal to it is related to visceral activity (Kimura et al., 2012; Stehberg et al., 2001). Limbic and motor systems are connected to sectors of the most rostral portion of the nuclei, with the motor sector also containing a somatotopic map (Cicirata et al., 1990; Gonzalo-Ruiz and Lieberman, 1995a, 1995b; Lozsadi, 1995, 1994).

Further, the connectivity between the Rt and different thalamic nuclei supports its division in three tiers along its thickness (e.g., see Fig. 1 for tiers specificity of VPL, VPM, and POm projections) (Clemente-Perez et al., 2017; Lee et al., 2014; Pinault, 2004; Pinault et al., 1995a). Differences in cell bursting behavior along the dorsoventral axis of the nuclei (non-bursting, bursting, or atypical bursting) has also been reported (Lee et al., 2007) and suggest regional variation in this nucleus not only in terms of cell densities but also in terms of cellular electrophysiological behavior (Fig. 7B).

5. Microconnectivity

Studying the connectivity patterns and the properties of synaptic

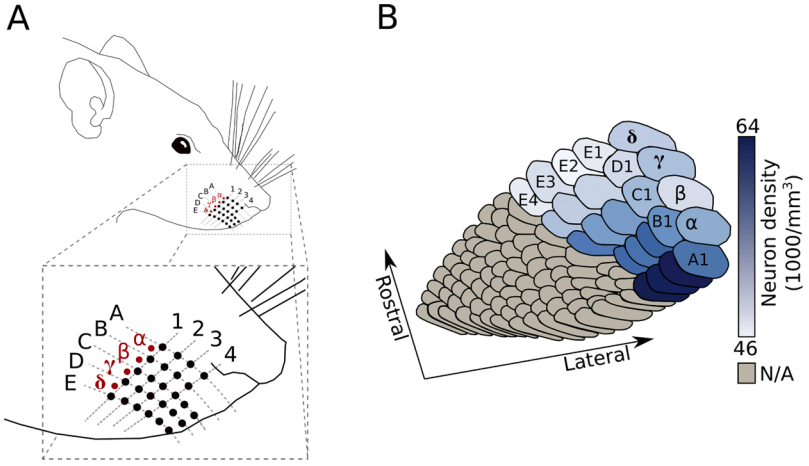

Fig. 6. Topological relationship between whiskers and barreloid in the rodent VPM. A) The snout of the rat with macrovibrissae arcs (A-E) and rows (1-4) in black and straddlers in red. B) Barreloids in the VPM, as represented by Haidarliu and Ahissar (2001) (reproduced with permission), with cellular densities per barreloid taken from Meyer et al. (2013). In grey, next to macrovibrissae rows are aggregates of neurons associated with microvibrissae, for which no density estimates are currently available.

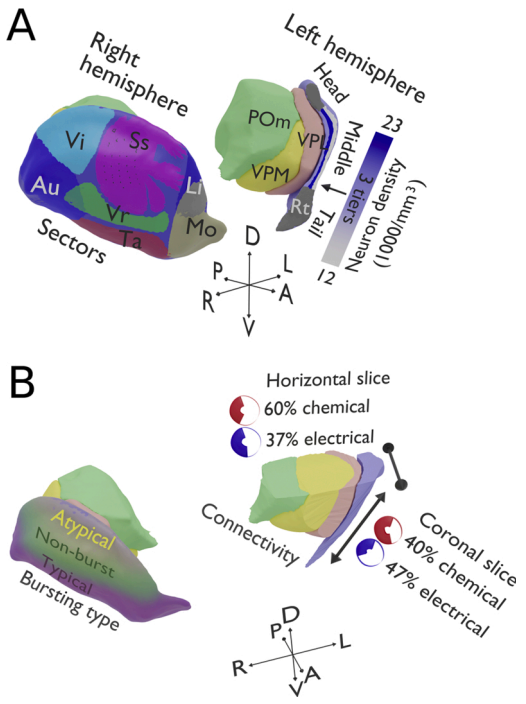

Fig. 7. Schematic representation of sources of topological variability within Rt, overlaid on the volumes of somatosensory thalamic regions, as parcellated by the Allen Mouse Brain Atlas. Thalamic regions are shown from the front side of the brain. Axis system: dorsal (D), ventral (V), right (R), left (L), anterior (A), and posterior (P). A) Right hemisphere (left side): Schematic representation of the topological organization of the Rt in the sectors most often described in the literature: somatosensory (Ss), visual (Vi), auditory (Au), visceral (Vr), taste (Ta), Limbic (Li), and motor (Mo). Somatotopy in the Ss sector is represented as proposed by Shosaku et al. (1984) (reused with permission). Although not represented here because of the lack of sufficiently precise descriptions, a similar topological organization can be observed across different modalities. Left hemisphere (right side): cut view of the somatosensory thalamus, including POm, VPM, VPL, and Rt. Rt is shown separated in head, tail, and tiers in the middle part. Cell densities (for adult rats) (Ross et al., 1995) in the different tiers are color-coded to highlight the heterogeneity of the cell composition across this nucleus. No cell density has been reported for the head and tail sections specifically. Connectivity, dendritic fields, and gap junctions networks have also been shown to depend on tiers (not represented here). B) Right hemisphere (left side): Schematic representation of the electrophysiological behavior of Rt cells varying along the dorsoventral axis (Lee et al., 2007). Left hemisphere (right side): Percentage of coupled cells depends on the plane in which the connectivity is probed with more electrical connectivity along the dorsoventral direction in coronal slices and more chemical connectivity along the anteroposterior direction in horizontal slices (numbers for P12-P15 rats from Deleuze and Huguenard (2006)).

connections is necessary for understanding and modeling the dynamics of TC interactions. For example, the reciprocal innervation of Rt and TC cells allows them to generate important rhythmic behavior (e.g., sleep spindles) through a ping-pong-like mutual activation (Lüthi, 2014). Such dynamics critically depend on microconnectivity patterns. These aspects are reviewed here for the microconnectivity within the TC system and in the next section for external afferents. Cortical efferents and their laminar specificity are covered in Section 3.1.2 in the context of axonal morphology.

5.1. Connectivity patterns

As a rule, FO TC cells do not send collaterals within the dorsal thalamus. Some rare cases of lateral connections have been reported in young animals, but these connections are thought to be pruned during maturation (Lee et al., 2010). TC cells from cat LGN have been shown to send intranuclear collaterals that form synapses onto intralaminar interneurons[2] (Cox et al., 2003) and potentially even to other TC cells (Soltesz and Crunelli, 1992). However, the presence of such collateral has not been supported experimentally for other nuclei or for rodent species (Harris, 1987; Sawyer et al., 1994).

TC cells target directly extrathalamic (e.g., cortical) areas, sending collaterals to the Rt on their way to the cortex. The Rt projects back inhibitory input onto FO (and other) nuclei, creating either 1) a disynaptic inhibitory feedback loop, 2) a disynaptic center-surround type of local lateral inhibition or 3) a disynaptic lateral inhibition between nuclei of the dorsal thalamus (Guillery and Harting, 2003; Kimura et al., 2007).

The literature suggests a certain number of basic rules related to microconnectivity in the thalamus:

1 TC cells do not project within their nucleus.
2 TC cells do not project directly to other nuclei of the dorsal thalamus.
3 Rt cells do not have other external targets than the dorsal thalamus.
4 Thalamic interneurons project only within their nucleus.

From a theoretical point of view, these four rules eliminate a good number of possible connection patterns and leave 18 possible disynaptic or trisynaptic pathways for a TC cell to provide feedback to itself (intra-nucleus, closed-loop), to a neighboring TC cell (intra-nucleus, open-loop), or to a TC cell of another nucleus (inter-nucleus). Each of these combinations (i.e., intra vs. inter-nucleus, closed vs. open-loop, disynaptic versus trisynaptic) can have an inhibitory or excitatory impact, considering disinhibition as providing an overall excitatory impact (Fig. 8).

Information about the relative proportion of these different connection patterns is key for understanding and modeling the TC system. Even when they constitute an emergent property of a modeling approach (e.g., deriving connections from appositions of realistic morphologies as in Hill et al. (2012)), these proportions are required for model validation. Relatively few studies report such figures, except for patterns 1 (closed thalamo-reticular loop) and 3 (open thalamo-reticular loop) for which proportions have been reported both structurally and functionally (see Table 2; Gentet and Ulrich, 2003; Lee et al., 2010; Lo and Sherman, 1994; Pinault and Deschênes, 1998b; Shosaku, 1986). Such proportions need to be assessed both structurally and functionally since these two types of connectivity are linked through an intricate relationship. Many factors are involved in how structural connections support functional interactions, such as the strength of the synaptic connections, cellular electrophysiological properties, or time-frequency patterns of incoming activity. For example, at low frequency, the combination of patterns 2 and 9 produces a very short excitation (pattern 2) followed by inhibition (pattern 9). However, at high frequency, this combination produces only excitation because of short-term facilitation in the corticothalamic synapses and short-term depression in the reticulo-thalamic pathway (Crandall et al., 2015).

5.2. Chemical synapses

5.2.1. Rt-TC synapses

The strength of reticular inhibitory connections to VB in paired recordings is very variable (inhibitory postsynaptic current (IPSC) amplitude range: 18.5–514.0 pA; latency: 1.5–3.1 ms) and depends on various factors such as the proportion of postsynaptic failures, the amplitude of unitary IPSCs, and the density of axonal swellings. It is qualified as either weak (conductance: 0.46 ± 0.14 nS; range 0.35−0.61 nS) or strong (conductance: 4.5 ± 4.6 nS; range: 1.85–12.7 nS) (Cox et al., 1997). Each synaptic contact generates a unimodal (mean

[2] As opposed to cats, nocturnal rodents do not show clear lamination in the LGN (Monavarfeshani et al., 2017).

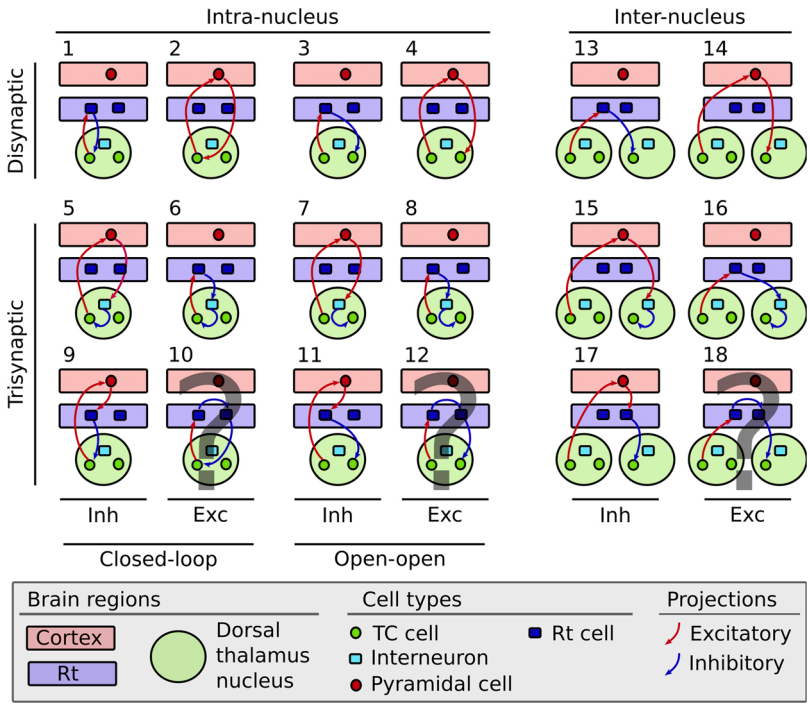

Fig. 8. All possible connectivity patterns from one TC cell to itself or to another TC cell in at most three synapses according to the four rules previously listed. Grey interrogation marks have been superimposed over patterns involving Rt-Rt chemical connections since evidence about their existence in adult rodents is equivocal (Section 5.2.2). Rt-Rt connections through electrical synapses (Section 5.4) are not represented in this figure. Inh: Inhibition; Exc: Excitation or disinhibition.

Table 2
Prevalence of open versus closed thalamo-reticular loops.

Prevalence of open-loop	Sample size	Animals	Region	Type of experiment	reference
84 %	86	Adult rats	AD(1), AV(1), LD/LP (5), MD (1), Po (1), VL (8), VB (5)	Anatomical	Pinault and Deschênes (1998b)
93 %	14	Juvenile (P14-P20) rats	VB	Physiological	Gentet and Ulrich (2003)
79 %	34	Rats	VB	Physiological	Shosaku (1986)
83 %	36	Adult cats	LGN	Physiological	Lo and Sherman (1994)

amplitude 12.2 ± 1.3 pA) or a bimodal (mean 13.2 ± 6.3 pA and 24.2 ± 16.8 pA) distribution of miniature IPSC (mIPSC) amplitudes (Cox et al., 1997).

VB responses from reticular inhibition can last up to hundreds of milliseconds and typically display an early Cl^--mediated $GABA_A$ component and a late K^+-mediated $GABA_B$ component of about 20 % the amplitude of the $GABA_A$ component (Huguenard and Prince, 1994). Compared to other cells, the $GABA_A$ reversal potential in TC cells is very negative, suggesting the existence of a mechanism extruding Cl^- (Huguenard and Prince, 1994).

When compared with $GABA_A$-mediated mIPSCs recorded in dLGN TC cells, mIPSCs in VB TC cells have faster kinetics (VB: 1.4 ± 0.2 ms, dLGN 1.7 ± 0.5 ms rise times; VB: 18.6 ± 3.6 pA/ms, dLGN: 14.8 ± 5.2 pA/ms decay slopes) and narrower half-widths (VB: 8.19 ± 1.46, dLGN: 11.6 ± 3.5 ms), but similar amplitudes (VB: 25.9 ± 0.89 pA, dLGN: 29.4 ± 0.8 pA) (Yang et al., 2017). The slower rise time and longer half-widths of mIPSC are characteristics of dendritic release from dLGN interneurons and may be due to differences in the subunit composition of their $GABA_A$ receptors. This suggests that the reported differences between mIPSCs in VB and dLGN TC cells may be attributed to a larger contribution from interneurons in the dLGN (Yang et al., 2017).

5.2.2. *TC-Rt synapses*

The Rt receives excitatory inputs from TC and CT axons, with the latter accounting for ~60 % of the total excitatory terminals (Liu and Jones, 1999), in line with previous reports showing much denser CT than TC projections (Deschênes et al., 1998; Sherman and Koch, 1986). These two types of input can be distinguished by their short-term dynamics: L6 CT synapses onto Rt neurons are facilitating, while TC axons are depressing (Astori and Lüthi, 2013; Gentet and Ulrich, 2003; Golshani et al., 2001).

TC-Rt synapses in VB generate strong excitatory postsynaptic potentials (EPSP; amplitudes [mean ± SEM]: 7.4 ± 1.5 mV, range 0.7−27 mV), few synaptic failures, and low variability of the kinetic properties and synaptic latencies (rise time: 0.63 ± 0.03 ms; decay time: 15.12 ± 0.91 ms) (Gentet and Ulrich, 2003). Similar EPSP amplitudes (0.5–2.0 mV in Rt neurons held between –70 and –80 mV) and short-term depression were found in dLGN TC neurons of ferrets (Kim and McCormick, 1998).

Depending on the baseline potential, AMPA contributes between 68.1 ± 4.9 % and 71.4 ± 4.1 % of the total EPSP in the VB TC-Rt synapses of juvenile (P14-P20) rats (Gentet and Ulrich, 2003). This contribution changes during development, with NMDA/AMPA ratio decreasing from 0.42 at P14 to 0.27 at P21-P28 in mice (Astori and Lüthi, 2013). Although this indicates synaptic maturation, NMDA receptors in Rt neurons continue to express GluN2B instead of seeing it substituted by GluN2A as it is usually the case during development (Astori and Lüthi, 2013).

VB TC-Rt synapses may also contain a rare type of NMDA receptor subunit not requiring depolarisation to remove the Mg^{2+} block since only a low proportion of NMDA receptors are blocked at resting

membrane potentials lower than −70 mV (Gentet and Ulrich, 2003).

5.2.3. Rt intrinsic connections

Recurrent inhibition in Rt is controversial. Some studies in rats report relatively frequent recurrent connections: 40%–60% at P12-P15 (Deleuze and Huguenard, 2006); 62 % (N = 47) at P10-P12 (Lam et al., 2006). However, other studies found these connections to be rare (2.8 % incidence of inhibitory connections (N = 180) in P4-P8 mice (Parker et al., 2009)) or absent (in P12-P21 rats (Landisman et al., 2002; Long et al., 2004)). Recent optogenetic experiments in mice suggest that these connections are pruned within the first two weeks after birth (Hou et al., 2016). However, other investigators, also using optogenetic stimulation, found weak but present Rt-Rt connections in 2–4 months old mice (Makinson et al., 2017). Reciprocal inhibitory connections in Rt have been hypothesized to help desynchronize Rt activity in context of sleep and epilepsy (Huntsman et al., 1999). GABAergic terminals in Rt account for about 10 % of all connections to the Rt (Guillery and Harting, 2003) but it is currently unclear what proportion of these terminals come from external afferents (e.g., ZI, basal forebrain, globus pallidus, pretectum; see Section 6.3) or from recurrent Rt connections.

5.2.4. Interneurons synapses

Electron microscopy studies have shown that interneuron dendrites together with incoming retinal ganglion axons form a triadic synapse onto TC dendrites (Hamos et al., 1985; Morgan and Lichtman, 2020; Section 5.2.5). The F2 terminals of these interneurons have been shown to be associated with two types (A and B) of feedforward inhibitory responses depending on their receptors. Although every F2 terminal has AMPA and NMDA receptors, only those exhibiting the type B response also contain type 5 metabotropic glutamate receptors (mGluR5) which cause longer-lasting feedforward inhibition. Both types of response were observed in the same postsynaptic cells, and these cells were morphologically different from those not displaying any response typical of F2 terminals (Crandall and Cox, 2013).

The amplitude and duration of IPSCs caused by interneuron spikes depend on the contribution of sodium and calcium conductances. In presence of TTX, sodium spikes of axonal and dendritic origin cause rapid $GABA_A$ IPSCs (10%–90% rise time: 1.2 ms) whereas dendritic calcium spikes generate slow IPSCs (10%–90% rise time > 20 ms) at the interneurons-TC synapse (Acuna-Goycolea et al., 2008). These differences indicate that these interneurons may rely on a variety of inhibitory signaling mechanisms.

There is some anatomical evidence from electron microscopy that Rt to local interneuron synapses exist (Morgan and Lichtman, 2020). Further, LGN interneurons in rats have been shown to receive IPSPs when the Rt is extracellularly stimulated. These IPSPs are mediated only by bicuculline-sensitive $GABA_A$ receptors expressed by the interneurons (Zhu and Lo, 1999b).

5.2.5. Glomeruli, triadic synapses, and local connectivity motifs

Triadic synapses insulated by sheaths of astrocytic processes form glomerulus-like arrangements in the thalamus (Sherman, 2004; Spacek and Lieberman, 1974). These triadic synapses allow ascending glutamatergic driving inputs to trigger fast feedforward inhibition onto proximal TC dendrites by directly releasing GABA from interneurons dendrites (i.e., dendro-dendritic contacts; Fig. 9A). Compared to non-triadic configurations, these synapses provide faster (~1 ms delay) and more reliable feedforward inhibition (Blitz and Regehr, 2005).

Because they involve interneurons, triadic synapses have been studied mostly in the LGN, where they have been shown to modulate driving inputs by controlling their gain (Heiberg et al., 2016; Sherman, 2004) and by inducing a response lag (Vigeland et al., 2013). They also sharpen the temporal precision of incoming information by generating short windows of excitatory input on TC cells, i.e., an initial monosynaptic excitation followed 1 ms later by disynaptic feedforward inhibition mediated by interneurons (Babadi et al., 2010; Butts et al., 2011; Casti et al., 2008).

As opposed to modulatory L6 afferents that target distal TC dendrites with small non-glomerular synapses (Guillery and Sherman, 2002), L5 afferents can drive thalamic activity through glomerular synapses formed on proximal dendrites of HO TC cells (Hoogland et al., 1991; Rouiller and Welker, 1991). These glomerular arrangements further enable L5 afferents to trigger a feed-forward inhibition of TC cells through incerto-thalamic terminals (Bartho et al., 2002).

Interestingly, a single LGN thalamic interneuron creates diverse types of connectivity motifs, such as those illustrated in Fig. 9B-F as well as various other chain variants of these motifs not shown (Morgan and Lichtman, 2020). This suggests that the interneurons hold very complex computational properties and may be responsible for shaping incoming sensory stimuli. Computational simulations of such circuitry could serve as a helpful tool to parse out these sophisticated microcircuitries.

5.3. Electrical synapses

Gap junction (GJ) protein connexin36 is known to be highly expressed in Rt (Liu and Jones, 2003). Both connexin36 and connexin45 are also expressed in VB TC cells, where they play a role in the early development of chemical synapses and gradually disappear during the first postnatal week (Lee et al., 2010; Zolnik and Connors, 2016). GJ protein Pannexin1 has also been reported in the thalamus (Cone et al., 2013), particularly in Rt cells (Ray et al., 2005; Zappala et al., 2006), but it may not be contributing to electrical coupling (Huang et al., 2007; Lee et al., 2010).

Rt GJs create a strong electrical coupling between Rt cells (Blethyn et al., 2008; Landisman et al., 2002; Long et al., 2004) and support the reticular rhythmogenesis by synchronizing neuronal activity (Long et al., 2004), similar to what was observed in GJ-connected cortical inhibitory neurons (Deans et al., 2001). Although both chemical and electrical synapses may be involved in different functions such as the synchronization of cell assemblies in the Rt of young rodents (Deleuze and Huguenard, 2006), the coupling remaining in adult rodents is mostly due to electrical synapses (Hou et al., 2016; Makinson et al., 2017).

Different types of GJs-connected cell clusters (~15 % elongated, ~45 % discoid, and ~40 % spherical) may support functionally distinct networks in Rt (Lee et al., 2014). Elongated and discoid clusters tend to be constrained within single Rt tiers, spreading up to 30 % of the thickness of the nucleus. Accordingly, these types of clusters were

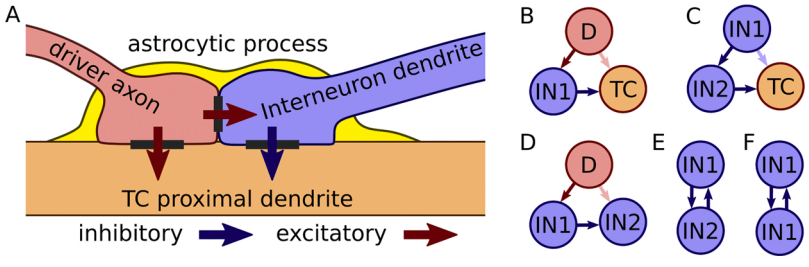

Fig. 9. Schematic representation of triadic synapses and local connectivity motifs. A) A triadic synapse ensheathed in an astrocytic process. B-F) Examples of various connectivity motifs involving interneurons that have been observed (Morgan and Lichtman, 2020). Paler arrows indicate optional connections, i.e., meaning that both the motifs with and without such a connection exist. Most of the connections from interneurons are dendro-dendritic. D: Driver afferent; IN1, IN2: Two different interneurons; TC: Thalamocortical relay cell.

reported to project to a single target (i.e., either POm or VB). That contrasts with spherical clusters that span up to 60 %–70 % of Rt thickness, covering multiple tiers which project to both POm and VB (see Fig. 1). The relationship between these types of clusters and the morphological subtypes of Rt cells (see Section 3.1.1) is currently unclear and should be elucidated in order to establish whether the shape of these clusters is an emerging property of the cellular composition or if a distinct mechanism is responsible.

Neurons with inter-somatic distance up to 300 μm were shown to be coupled through GJ using dye-coupling imaging (Lee et al., 2014). By contrast, paired recordings show connections only for neurons separated by inter-somatic distances up to 40 μm (Long et al., 2004). However, in this technique, the sampling volume increases rapidly with inter-somatic distances, quickly reducing probabilities of successfully finding connected pairs. Clusters of GJ connected Rt cells obtained with dye-coupling were found to include many, but not all cells with short inter-somatic distances, suggesting selective connectivity within the space spanned by these clusters (Lee et al., 2014).

Rt neurons were found to be connected through gap junctions with 8 ± 2.5 (range: 1–24; N = 9) neighbors when using dye-coupling. However, these figures are likely to be underestimated due to limited diffusion of dye through gap junctions, as indicated by lower coupling prevalence at short inter-somatic distances when compared with paired recordings. Using photostimulation, between 17 % and 47 % of Rt neurons were reported to be locally connected through GJs (Deleuze and Huguenard, 2006; Lam et al., 2006).

By introducing electrical coupling, GJs allow the low-frequency subthreshold activity to move across Rt cell networks (Bennett, 1966; Connors and Long, 2004). Membrane passive properties result in low-pass filtering of this activity, with stronger high-frequency attenuation early in development due to a nearly four times higher membrane time constant at P1 (72 ± 4 ms) compared to P14 (19 ± 1 ms) in mice (Parker et al., 2009).

Coupling coefficient of 0.12 ± 0.08 (N = 313) and synaptic conductance of 0.80 ± 0.63 nS (N = 313) have been reported for Rt GJs (Haas et al., 2011). However, long-term depression (LTD) can modulate the strength of this coupling. Two mechanisms can trigger such LTD: 1) simultaneous bursting in coupled neurons (Haas et al., 2011) and 2) activation of metabotropic glutamate receptors from cortical input (Landisman and Connors, 2005). These two sources of plasticity act through distinct mechanisms, allowing intrinsic Rt activity and cortical afferents to independently fine-tune the strength of GJ (Sevetson et al., 2017). This LTD is sufficient to influence spike synchronization in coupled Rt cells (Landisman and Connors, 2005) and it modulates GJ coupling independently in both directions (Haas et al., 2011; Sevetson and Haas, 2015), providing a flexible mechanism for regulating the spread of rhythmic activity.

5.4. Closed and open-loops

The proportion of connections forming open or closed loops is a fundamental characteristic of the TC microconnectivity (Halassa and Acsády, 2016). The degree of convergence (closed-loop; feed-back inhibition) or divergence (open-loop; lateral inhibition) of information propagation in the system depends on the relative proportion of these patterns. Since most of the thalamus has a topological structure, the degree of divergence or convergence is likely impacting on the sharpness of stimuli (e.g., the resolution for the localization of a touch stimulus) and on selective attention.

This topic has been more often studied in the thalamo-reticular loop than in the TC loop, probably because it is challenging to track long-distance projections between the thalamus and the cortex. The thalamo-reticular network comprise a mix of open and closed-loop connections (Deschênes et al., 1998; Desilets-Roy et al., 2002; Halassa and Acsády, 2016; Lam and Sherman, 2005; Pinault and Deschênes, 1998b; Rouiller and Welker, 2000), with a dominance of 80 %–90 % of open-loop connections (see Table 2). However, the number of closed-loop connections may be underestimated due to severed connections in sliced preparations. The thalamus probably needs to fine-tune this degree of divergence to generate TC rhythms (e.g., sleep spindles) that do not degenerate in uncontrolled oscillations (e.g., epileptic activity). A proper degree of divergence is required for populations of cells to be recruited and initiate population rhythmic activity (waxing), to limit their spatial spread, and to timely desynchronize cell assemblies (waning) (Pita-Almenar et al., 2014).

At the level of the TC loop, small (<1 μm) and giant (2–10 μm) CT axon terminals are involved in different functional networks. Small terminals provide cortical feedback and are more likely to form closed-loop, whereas giant terminals are passing along feed-forward signals through cortico-thalamo-cortical routes (Rouiller and Welker, 2000). Because of their focal and topologically accurate projection patterns, core TC cells from FO are likely to participate in a higher proportion of closed-loop circuits. By opposition, the greater spread of matrix TC projections from HO is likely to support a larger proportion of open-loop circuit associated with feed-forward cortico-thalamo-cortical communication and a lower proportion of closed-loop connections providing feedback to CT cells (Clasca et al., 2012).

6. Afferents

Thalamic afferents need to be carefully considered for both experimental and modeling work in the TC system since they are closely related with behavioral differences in subpopulation of thalamic cells. By considering the direction of the flow of neural information, we can categorize thalamic afferents as being either ascending (from sensory inputs to percepts) or descending (from mental representation to motor actuators). To some extent, the patterns of afferent pathways can be generalized across modalities by considering FO/HO and driver/modulatory properties of the nuclei and the afferents. However, because there are also many details that are specific to every sensory modality, our review of thalamic afferents is limited to the somatosensory system.

6.1. Ascending projections for the somatosensory system

The major afferent pathways for the rodent somatosensory system are depicted in Fig. 10. The VPL and VPM receive input from sensory cells through two main pathways: the lemniscal and the extralemniscal. For the region of the head, the lemniscal pathway goes through the trigeminal ganglion and forms synapses in the principal nucleus of the trigeminal complex (Pr5). Then it crosses contra-laterally and passes through the trigeminal lemniscus to reach the VPMdm (Pierret et al., 2000; Veinante et al., 2000). For the rest of the body, first-order neurons have their somata in the dorsal ganglion root and project along the dorsal column to the brainstem where they synapse to cells in the gracile (lower body) or the cuneate (upper body) nuclei. Axons of these second-order neurons cross contra-laterally and climb up through the medial lemniscus, which projects to VPL, most heavily to its rostral portion. This route is also named the dorsal column-medial lemniscus pathway. It is the main pathway for fine touch, vibration, two-point discrimination, and proprioception. It is fast, precise, and phylogenetically recent (Ebner and Kaas, 2015).

The extralemniscal pathway is also called neospinothalamic or spinothalamic (Yu et al., 2006) and is part of the anterolateral or ventrolateral system. It is associated with nociception (pain) and dull sensations, such as crude touch and temperature sensation. It reaches the spine through the dorsal ganglion root, crosses to the contralateral side, and climbs up through the ventral and lateral spinothalamic fasciculi to project to VPL, most heavily to its caudal portion. Similarly, for the head, the analog pathway passes through the trigeminal ganglion, then the spinal trigeminal complex (Sp5), most importantly through the interpolar division (see Veinante et al. (2000) for characterization of these projections separately for the oral (Sp5o), interpolar

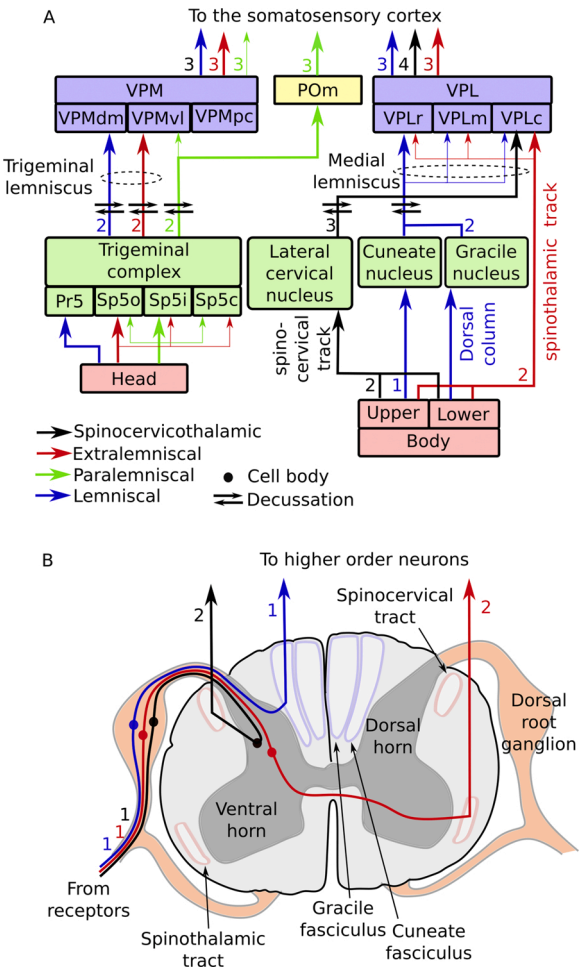

Fig. 10. Major ascending pathways for the somatosensory system of the rodent. A) High-level representation of the neural paths from the periphery up to the somatosensory cortex. B) Detailed view of the pathways at the spinal level. The numbers indicate the order of the neurons involved at each step of the pathways.

(Sp5i) and caudal (Sp5c) divisions). Then, it reaches the VPMvl (Pierret et al., 2000; Veinante et al., 2000) through the contralateral anterior division of the trigeminal lemniscus. Although terminals from the Sp5 (spinothalamic) and Pr5 (lemniscal) have been reported to be indistinguishable within VPM, they have been found to target distal and proximal dendrites, respectively (Williams et al., 1994).

A third pathway, the spinocervicothalamic (also named only spinocervical) pathway, is much less often discussed and generally only in the context of nociception. Contrary to the other trisynaptic pathways, it has four synapses. Cells from the dorsal root ganglion form synapses onto neurons of the spinal dorsal horn. Then, spinal neurons project to the ipsilateral lateral cervical nucleus. Cervical projections cross contralaterally and project through the medial lemniscus to the most caudal part of VPL (Giesler et al., 1988).

Another important ascending somatosensory pathway, the paralemniscal pathway, projects to Sp5, and more particularly to the Sp5i. It involves Sp5i large soma cells with thick and fast conducting axons, as opposed to the spinothalamic projections from Sp5i, which project thin and slow conducting axons from smaller cells (Pierret et al., 2000; Veinante et al., 2000). It reaches the PO directly and also targets the non-barreloid VPMvl region (Williams et al., 1994). It is associated with nociception (Frangeul et al., 2014) and contains poorly segregated information. For example, as opposed to the lemniscal pathway, for which specific input has strong single-whisker dominance (Gauriau and Bernard, 2004; Pierret et al., 2000), this pathway contains multi-whisker information (Williams et al., 1994). As opposed to lemniscal inputs to VPM which are only of a driver type, the paralemniscal pathway projects to PO with a mix of driver (29 %) and modulatory (71 %) inputs (Mo et al., 2017). Feedforward inhibition from ZI inhibits this driving input to PO. Surprisingly, electrophysiological characterization has shown that disynaptic trigeminal-incertal-PO inhibitory input arrives earlier to PO than the monosynaptic trigeminal-PO excitatory input. These temporal properties explain the relatively low responsiveness of PO when it is only activated from this ascending driver input (Lavallée et al., 2005). However, PO cells are highly responsive when a paralemniscal input is shortly preceded by descending inputs (further discussed below; Groh et al., 2014).

Some other pathways associated with the somatosensory system, particularly for nociception, reach other parts of the thalamus, e.g., the pathway reaching the centromedian parafascicular nuclei of the thalamus from the anterior spinothalamic tract. We do not review these pathways here.

In summary, the pattern of ascending afferents is complex, with different pathways supporting different functions such as touch, proprioception, and nociception. The thalamic regions that these pathways target partially overlap, but are nevertheless characterized by modality and afference dominance (i.e., afferents are not perfectly segregated, nor are they homogeneously mixed within somatosensory thalamic nuclei). These different afferents evolved in steps, newer systems being added on top but in interaction with older systems. Most ascending afferents have large terminals with round vesicles, which partly distinguish them from Rt or CT afferents, but not between themselves. Further, some ascending afferents (e.g., lemniscal) exhibit a mixture of driver and modulatory properties, which complicates their segregation from cortical afferents based on synaptic physiology alone. However, VGluT1/VGluT2 immunohistochemistry can be used to distinguish brainstem and spinal cord inputs (VGluT2 positive) from cortical ones (VGluT1 positive) (Graziano et al., 2008).

6.2. *Descending projections for the somatosensory system*

Three distinct CT projections have been described, depending on their laminar origin: L5, L6a, or L6b (Hoerder-Suabedissen et al., 2018). To restrain the scope of this review, we focus on S1 projections, although other areas such as S2 and the motor cortex also project to the somatosensory thalamus (Rouiller et al., 1991). To facilitate the comparisons across these pathways, Table 3 provides a summary of some of their key properties.

As a population, L5 projections target more densely HO (e.g., POm) than FO (e.g., VB) (Hoerder-Suabedissen et al., 2018). L5 cells often

Table 3
Summary table for the properties of the descending afferents to the somatosensory thalamus.

	L5	L6a	L6b
Rt collaterals	No	Yes	No
Type	Driver for PO; Modulator for VB, except maybe at its fringes	Modulator	Modulator
Target VPL	Sparse collaterals with small varicosities;	Yes	It occasionally has a few collaterals
Target VPM	some large L5 varicosities in dorsal, medial, and ventral fringes of VB and in VPMvl	Yes	No direct collaterals; Sometimes dendrites travels back from PO
Target PO	Dense collaterals with small and large varicosities	Yes	Yes
Subcellular target	Proximal dendrites	Distal dendrites; colocalized with ascending input	

project only to HO (Bourassa et al., 1995; Reichova and Sherman, 2004; Veinante et al., 2000). The size of POm varicosities from L5 projections vary in a wide range, with some being relatively small (similar to those from L6) but also with a significant proportion being much larger (3–8 μm) (Bourassa et al., 1995; Hoerder-Suabedissen et al., 2018). Only small L5 varicosities have been reported in FO (Hoogland et al., 1991), except for some large L5 terminals found in the dorsal, medial, and ventral fringes of VB as well as in VPMvl (Liao et al., 2010). L5 cells project to the thalamus but not to the Rt (Bourassa et al., 1995; Bourassa and Deschenes, 1995). They do so through collaterals, their final target being regions of the brainstem (e.g., superior colliculus) and the spinal cord (Bourassa et al., 1995; Deschênes et al., 1994). Similarly to TC projections, synapses from L5 afferents have a fast conduction time (Miller, 1996) suggesting a feed-forward role (Rouiller and Welker, 2000).

Through its L5 afferents to the ZI (Mitrofanis and Mikuletic, 1999), the cortex can lift the powerful incertal feedforward inhibition of paralemniscal inputs to PO (e.g., passive whisker deflection) when they are co-occurring with top-down stimulation (e.g., active whisking) (Lavallée et al., 2005). Two mechanisms are available to the cortex for this: 1) by triggering auto-inhibition of ZI through its network of re-entering GABAergic collaterals (Bartho et al., 2002; Power and Mitrofanis, 1999) or 2) by cortical activation of the APT projections to ZI (Section 6.3; Giber et al., 2008).

As opposed to the driver afferents from L5 that targets proximal TC dendrites, L6 afferents are modulator and target distal TC dendrites. In the PO of rats and mice, synapses from L6 afferents have been shown to be colocalized with driving spinal trigeminal inputs, both afferents forming terminals close to one another (i.e., <5μm; Groh et al., 2014). This proximity allows PO to integrate ascending and descending streams, as supported by a supralinear gain for spiking probability when ascending input arrives within a time window spanning tens of milliseconds after the arrival of cortical activity.

Afferents from L6a project to both FO and HO with a similar density (Hoerder-Suabedissen et al., 2018) and provide feed-forward inhibition through their collaterals to Rt (Bourassa et al., 1995; Bourassa and Deschenes, 1995; Lam and Sherman, 2010). They project only to sensory-specific nuclei (Bourassa et al., 1995; Deschênes et al., 1998) and those from barrel columns project only to corresponding barreloids (Deschênes et al., 1998).

Some L6b cells have been shown to arborize in POm without any collaterals to either VB or Rt. A genetically labeled subset of CT axons from this layer of the somatosensory cortex has also been reported to arborize at the edge of POm, with some branches traveling back to VPM. As opposed to cells from L6a, they do not send collaterals to Rt and, in some cases, send collaterals to VPL, but not to VPM (Hoerder-Suabedissen et al., 2018). These may correspond to a small proportion of CT cells in the lower part of L6 that have been reported to arborize only in POm (Bourassa et al., 1995). Deep L6 projections have more frequently multinuclear innervation patterns. For example, they can target associative and/or intralaminar thalamic nuclei associated with given modalities. They also participate in the formation of rods or barreloids in specific nuclei (Deschênes et al., 1998). However, since L6a/L6b have not been clearly distinguished in earlier studies, it is difficult to unambiguously associate observations about lower/upper L6 with L6a/L6b. Further, the distinction observed within L6a and L6b may be different in granular versus dysgranular portion of S1 (Deschênes et al., 1998).

Typical indicators (i.e., ionotropic glutamate receptors and depressing synapses located close to cell bodies) show that L5 pyramidal cells from S1 provide POm with driving input. This is compatible with a feedforward role, i.e., this pathway carries information up the hierarchical network of the brain. By opposition, typical indicators (facilitating synapses on distal dendritic domains, with both ionotropic and metabotropic glutamate receptors) support a modulatory role for S1 L6a afferents to VPM. Therefore, this pathway is likely to transmit feedback down the brain hierarchy (Reichova and Sherman, 2004; Sherman and Guillery, 1996). Synapses from L6b require better characterization before similar roles can be attributed to this pathway (Hoerder-Suabedissen et al., 2018).

L6 CT projections are similar to cortico-cortical projections in that they are characterized by a highly variable conduction time, with some very long delays (Kelly et al., 2001; Kwegyir-Afful and Simons, 2009). By opposition, L5 CT (collaterals) have a fast conduction time, similar to the TC projections (Miller, 1996). The variable conduction time in L6 CT projections has been hypothesized to allow the modulation of the temporal dynamics of TC cells across time scales (Briggs and Usrey, 2008).

Synaptic variations suggest that these afferents have different spatial distribution within VB: the rostral part of this complex is innervated by small CT terminals, whereas its caudal region contains both small and large CT terminals. Further, this complex also contains a shell-like region that is characterized by large terminals (Liao et al., 2010).

Although in general, patterns of connectivity are similar across modalities, some differences exist. For example, in the auditory system, the FO (i.e., MGNv) has been shown to receive driving ascending input, whereas the HO (i.e., MGNd) is receiving ascending modulatory input (Lee and Sherman, 2010). Such segregation is less evident in the somatosensory system for which both driving and modulatory ascending afferents target POm (Mo et al., 2017).

6.3. External inhibition

Because most dorsal thalamic nuclei only have a small proportion of local inhibitory interneurons, a substantial part of their inhibition comes from external sources, mainly from Rt but also from other sources (Fig. 11).

ZI, a ventral thalamic region contiguous with Rt, and particularly its PV+ ventral portion, is an important source of inhibition for HO (Bartho et al., 2002; Bokor et al., 2005; Giber et al., 2008; Lavallée et al., 2005). It receives projections from L5 cells (Mitrofanis and Mikuletic, 1999) and from ascending afferents (e.g., from SpVi) (Lavallée et al., 2005), but not from the dorsal thalamus (Bartho et al., 2002). ZI innervates large proximal HO dendrites with clustered giant boutons (major axis up to 6–8 μm), establishing multiple release sites. These boutons form glomeruli with large excitatory boutons from L5 afferents (Bartho et al., 2002). Hence, ZI-thalamic inhibition seems to be very potent and focal, as opposed to Rt inhibition which is likely to have a more diffuse and

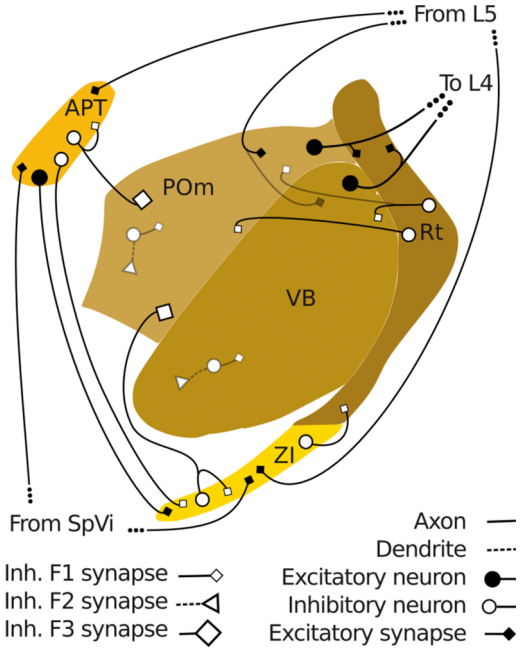

Fig. 11. Inhibitory circuits of the somatosensory thalamus.

modulatory effect (small boutons, generally single release sites, sparsely distributed across dendritic domains). ZI projections generally avoid small-size distal dendrites targeted by L5 projections (Bartho et al., 2002). Further, there is indirect but solid evidence that incertal but not Rt boutons have pre-synaptic type II muscarinic acetylcholine receptors. Although such receptors are nearly absent from VPL and VPM (except for the most caudal part), they constitute about half of the GABAergic terminals in PO, highlighting what is likely to be a considerable impact of ZI on the activity of this nucleus (Bartho et al., 2002).

Projections from the APT are very similar to those from ZI. They project only to HO forming large multi-synaptic boutons similar to incertal ones (Bokor et al., 2005; Giber et al., 2008; Lavallée et al., 2005) and designated as F3 terminals (Wanaverbecq et al., 2008) to emphasize their difference from F1 and F2 terminals found in the thalamus. As for ZI, and as opposed to Rt, APT has rich re-entrant GABAergic connectivity. However, as opposed to ZI, APT has similar connectivity with ascending and descending thalamic afferents (Lavallée et al., 2005) and sends no projections to Rt (Bokor et al., 2005; Cavdar et al., 2006).

APT and ZI are likely working in concert for controlling the activity in HO since APT projects to ZI with both GABA+ and GABA- boutons. Further, the APT-thalamic pathway is characterized by large and potent synapses (Bokor et al., 2005), whereas the APT-ZI pathway seems to have a milder modulatory effect and has smaller boutons with one or two synapses (Giber et al., 2008), suggesting a certain level of segregation between these two pathways. The existence of these parallel inhibitory pathways led to the proposal of an extrareticular system for the focal inhibitory control of HO, as opposed to a more modulatory control of the thalamus by Rt (Bokor et al., 2005). Nevertheless, this extrareticular system is likely to work in synergy with reticular inhibition since a ZI-Rt pathway has been reported in rats (Cavdar et al., 2006).

7. Outlook: gap and opportunities

7.1. A need for further data integration and system interoperability

Initial investigations of the TC system allowed establishing fundamental and structuring dichotomic concepts such as driver/modulatory afferents, FO/HO nuclei, core/matrix projections, and feed-forward/feedback inhibition. These concepts provide guidelines for extrapolating the vast amount of information required for understanding and modeling such a complex system using the unavoidably limited amount of observations that can be collected experimentally. In particular, although this review focuses on the somatosensory system, most properties of the TC loop in this system (e.g., the existence of a topological organization) can be generalized across sensory modalities and then fine-tuned to take into account peculiarities of given modalities.

To understand the biophysics of the TC loop, we can increasingly rely on high-resolution and high-throughput experimental recording methods. However, the potential of these new methods will be fully harnessed only if we manage to pool together quantitative experimental results from various sources. Such a pooling requires the experimental results to be systematically contextualize using open-access resources, like standard coordinate systems (e.g., the CCF (Oh et al., 2014)), atlases (e.g., the Waxholm Space Atlas of the Sprague Dawley Rat (Papp et al., 2014), the Allen Mouse Brain Connectivity Atlas (Oh et al., 2014)), ontological terms (e.g., the Neuroscience Information Framework Standard Ontology (Imam et al., 2012)), systematic curation of published data (O'Reilly et al., 2017), and interoperable neuroinformatics platforms (e.g., the Blue Brain Nexus; https://bluebrainnexus.io/). In particular, atlases containing point-to-point connection probabilities from experiments such as those stored in the Allen Mouse Brain Connectivity Atlas would prove invaluable. We also need to link spatial coordinates (i.e., not only whole brain regions) with quantitative values (i.e., not only dichotomic concepts) across cellular dimensions (e.g., electrophysiological behavior, morphological type, gene expression, protein expression), for example by embedding them as vectorial fields within shared spatial atlases. The fact that the topological variability shown in Fig. 7 could only be represented schematically rather than in a numerically accurate way is symptomatic of the absence of such resources. Since these results are not provided in a common spatial framework, they cannot be integrated accurately in a single space allowing cross-fertilization of studies (e.g., inferring the precise relationship between bursting types and somatotopy).

Reaching such a level of data integration is essential to tackle fundamental challenges associated with high experimental variability and low reproducibility, interspecies differences, complex developmental trajectories, and anomalies due to diseases and idiosyncratic conditions. Using standard frameworks to provide such a formal contextualization is necessary to support meta-analyses required to reach reliable conclusions from highly variable experimental results, as demonstrated here for cell densities (see Fig. 5). Unfortunately, not all required frameworks are yet available, and those currently existing often need ongoing improvements (e.g., better sub-parcellation of atlases, refinement of ontologies). The advent of the "big science" approach might support the costly and often under-appreciated development of such resources but will require deep cultural changes in our way to evaluate and reward scientific contribution and merit.

7.2. Outstanding knowledge gaps

A few outstanding gaps in our current knowledge are worth highlighting. For example, we have a rather shallow understanding of interneurons in other nuclei than LGN. Aside from the widely different proportions that have been reported in Section 4.3, almost nothing is known about their electrophysiological properties, their connectivity, their morphologies, and their functional role. Also puzzling is the report of non-GABAergic neurons in Rt (Cavdar et al., 2013). Further, only a few paired-recording studies have investigated comprehensively the inhibition between interneurons and TC cells, with none reporting on the dynamics of short-term plasticity associated with the IPSP at the interneuron-TC synapse. Similarly, little is known about reticular to interneuron connectivity in rodents.

Experimental and modeling investigation of the interaction between neurons and glial cells is necessary in order to characterize their impact on hemodynamics and foster a more complete understanding of neuronal dynamics. Although this aspect has been relatively understudied, it has recently received more attention and this trend is likely to increase as the neuroimaging community further models brain activity from blood oxygen levels measured by functional magnetic resonance imaging and similar recording modalities (Blanchard et al., 2016; Chander and Chakravarthy, 2012; Chhabria and Chakravarthy, 2016). More specifically concerning the TC loop, thalamic glial cells have also been the focus of very few studies, even though they have been recognized to serve important functional roles and to work in synergy with thalamic neurons. For example, they have been shown to disinhibit VB TC neurons (Copeland et al., 2017). VB glial cells have also been reported to form two classes, depending on their response to TC synaptic input, and they have been hypothesized to contribute to the processing of somatosensory information and the modulation of network activity (Parri et al., 2010). Unfortunately, reliable modeling of neuro-glio-vascular interactions will only be possible after these cells are experimentally characterized in much more detail.

Further quantitative and high-resolution information about connectivity is also necessary for neurons involved in the TC loop. It is challenging, with the current state of the art, to infer a precise and comprehensive picture of how synaptic boutons are distributed within thalamic nuclei and individual morphologies. Without this information, connectivity within biophysically-detailed models can only be roughly approximated, with undetermined consequences on network activity. Much more information is also needed to derive precise space-aware estimations of the prevalence of the microconnectivity patterns

described in Fig. 8. These need to be assessed not only structurally, but also functionally since they are likely modulated by CT activity, e.g., by facilitating the response of a group of cells through NMDA spikes or by inhibiting a group through extrareticular pathways.

7.3. Future perspectives

On the bright side, impressive methodological developments are promising fast progress on long-standing issues. For example, the sparsity and variability in stereological studies reporting cell densities (Keller et al., 2018) is likely to be resolved by whole-brain approaches relying on novel techniques such as brain clearing (Kim et al., 2017; Murakami et al., 2018). Also, high-throughput whole-brain sparse labeling and imaging of brain cells should greatly improve the thoroughness of our cell morphology sampling (Gong et al., 2016) and will support the reconstruction of much more complete (i.e., not cut by the slicing performed during patch-clamp experiments) morphologies (Economo et al., 2016; Reardon, 2017). For example, the MouseLight project at the Janelia Research Campus has recently made available 1,000 complete cell morphologies, with long range axonal projections spanning large portions of the mouse brain (Winnubst et al., 2019). The availability of morphologies with complete axonal projections will be invaluable for large-scale modeling and may have a profound impact on our way to view the TC system.

Furthermore, since its introduction over a decade ago, optogenetics has allowed researchers to design in vivo experimental protocols that provided a strong foundation to decorticate neuronal networks in more natural conditions (Deisseroth, 2015). These advances have been further supported by the recent development of miniaturized imaging equipment, such as miniscope and gradient-index (GRIN) lenses (Ghosh et al., 2011), which made calcium imaging possible in freely behaving animals (Zhang et al., 2019). Similarly analyzing extracellular potentials with Neuropixel probes (Jun et al., 2017), will likely improve significantly our understanding of dynamics in the TC loop during its normal mode of operation. With these in vivo experimental tools, we can now probe the inner workings of sleep, sensory processing, and behavior. These new methods are likely to help us shed a new light on cellular- and network-level mechanisms involved in diseases associated with abnormal thalamic rhythmogenesis, as previously reported for conditions like epilepsy, schizophrenia, and autism. Combined with fast-paced improvement in modeling methodologies and the steady increase of available computational power, these experimental advances are paving the way for great leaps in our understanding of the TC system.

Declaration of Competing Interest

None.

Acknowledgments

This research has been supported by McGill's Azrieli Centre for Autism Research (ACAR) and the Fonds de recherche du Québec – Santé (FRQS), the Krembil Foundation, and by general funding from the ETH Board of the Swiss Federal Institutes of Technology to the Blue Brain Project of the École polytechnique fédérale de Lausanne. We want to thank Nicolas Antille for generating Fig. 2 and Karin Holm for helping to proofread the manuscript.

References

Abbas, S.Y., Ying, S.-W., Goldstein, P.A., 2006. Compartmental distribution of hyperpolarization-activated cyclic-nucleotide-gated channel 2 and hyperpolarization-activated cyclic-nucleotide-gated channel 4 in thalamic reticular and thalamocortical relay neurons. Neuroscience 141, 1811–1825. https://doi.org/10.1016/j.neuroscience.2006.05.034.

Acuna-Goycolea, C., Brenowitz, S.D., Regehr, W.G., 2008. Active dendritic conductances dynamically regulate GABA release from thalamic interneurons. Neuron 57, 420–431. https://doi.org/10.1016/j.neuron.2007.12.022.

Ahissar, E., Oram, T., 2015. Thalamic relay or cortico-thalamic processing? Old question, new answers. Cereb. Cortex N. Y. N 1991 (25), 845–848. https://doi.org/10.1093/cercor/bht296.

Ahrens, S., Jaramillo, S., Yu, K., Ghosh, S., Hwang, G.-R., Paik, R., Lai, C., He, M., Huang, Z.J., Li, B., 2015. ErbB4 regulation of a thalamic reticular nucleus circuit for sensory selection. Nat. Neurosci. 18, 104–111. https://doi.org/10.1038/nn.3897.

Alloway, K.D., Hoffer, Z.S., Hoover, J.E., 2003. Quantitative comparisons of corticothalamic topography within the ventrobasal complex and the posterior nucleus of the rodent thalamus. Brain Res. 968, 54–68.

Ananthanarayanan, R., Esser, S.K., Simon, H.D., Modha, D.S., 2009. The cat is out of the bag: cortical simulations with 109 neurons, 1013 synapses. In: Proceedings of the Conference on High Performance Computing Networking, Storage and Analysis, SC' 09. ACM, New York, NY, USA, pp. 63:1–63:12. https://doi.org/10.1145/1654059.1654124.

Antic, S.D., Zhou, W.-L., Moore, A.R., Short, S.M., Ikonomu, K.D., 2010. The decade of the dendritic NMDA spike. J. Neurosci. Res. 88, 2991–3001. https://doi.org/10.1002/jnr.22444.

Anticevic, A., Cole, M.W., Repovs, G., Murray, J.D., Brumbaugh, M.S., Winkler, A.M., Savic, A., Krystal, J.H., Pearlson, G.D., Glahn, D.C., 2014a. Characterizing thalamo-cortical disturbances in schizophrenia and bipolar illness. Cereb. Cortex 24, 3116–3130. https://doi.org/10.1093/cercor/bht165.

Anticevic, A., Yang, G., Savic, A., Murray, J.D., Cole, M.W., Repovs, G., Pearlson, G.D., Glahn, D.C., 2014b. Mediodorsal and visual thalamic connectivity differ in schizophrenia and bipolar disorder with and without psychosis history. Schizophr. Bull. 40, 1227–1243. https://doi.org/10.1093/schbul/sbu100.

Aquino-Cias, J., Belceva, S., Bureś, J., Fifková, E., 1966. The influence of thalamic spreading depression on cortical and reticular unit activity in the rat. Brain Res. 1, 77–85. https://doi.org/10.1016/0006-8993(66)90106-5.

Arai, R., Jacobowitz, D.M., Deura, S., 1994. Distribution of calretinin, calbindin-D28k, and parvalbumin in the rat thalamus. Brain Res. Bull. 33, 595–614. https://doi.org/10.1016/0361-9230(94)90086-8.

Arcelli, P., Frassoni, C., Regondi, M.C., De Biasi, S., Spreafico, R., 1997. GABAergic neurons in mammalian thalamus: a marker of thalamic complexity? Brain Res. Bull. 42, 27–37.

Astori, S., Lüthi, A., 2013. Synaptic plasticity at intrathalamic connections via CaV3.3 T-type Ca2+ channels and GluN2B-containing NMDA receptors. J. Neurosci. Off. J. Soc. Neurosci. 33, 624–630. https://doi.org/10.1523/JNEUROSCI.3185-12.2013.

Astori, S., Wimmer, R.D., Prosser, H.M., Corti, C., Corsi, M., Liaudet, N., Volterra, A., Franken, P., Adelman, J.P., Lüthi, A., 2011. The Ca(V)3.3 calcium channel is the major sleep spindle pacemaker in thalamus. Proc. Natl. Acad. Sci. U. S. A. 108, 13823–13828. https://doi.org/10.1073/pnas.1105115108.

Astori, S., Wimmer, R.D., Lüthi, A., 2013. Manipulating sleep spindles–expanding views on sleep, memory, and disease. Trends Neurosci. 36, 738–748. https://doi.org/10.1016/j.tins.2013.10.001.

Augustinaite, S., Kuhn, B., Helm, P.J., Heggelund, P., 2014. NMDA spike/plateau potentials in dendrites of thalamocortical neurons. J. Neurosci. Off. J. Soc. Neurosci. 34, 10892–10905. https://doi.org/10.1523/JNEUROSCI.1205-13.2014.

Babadi, B., Casti, A., Xiao, Y., Kaplan, E., Paninski, L., 2010. A generalized linear model of the impact of direct and indirect inputs to the lateral geniculate nucleus. J. Vis. 10, 22. https://doi.org/10.1167/10.10.22.

Baran, B., Karahanoğlu, F.I., Mylonas, D., Demanuele, C., Vangel, M., Stickgold, R., Anticevic, A., Manoach, D.S., 2019. Increased thalamocortical connectivity in schizophrenia correlates with sleep spindle deficits: evidence for a common pathophysiology. Biol. Psychiatry Cogn. Neurosci. Neuroimaging 4, 706–714. https://doi.org/10.1016/j.bpsc.2019.04.012.

Bartho, P., Freund, T.F., Acsady, L., 2002. Selective GABAergic innervation of thalamic nuclei from zona incerta. Eur. J. Neurosci. 16, 999–1014.

Bartlett, E.L., Smith, P.H., 1999. Anatomic, intrinsic, and synaptic properties of dorsal and ventral division neurons in rat medial geniculate body. J. Neurophysiol. 81, 1999–2016.

Bennett, M.V., 1966. Physiology of electrotonic junctions. Ann. N. Y. Acad. Sci. 137, 509–539. https://doi.org/10.1111/j.1749-6632.1966.tb50178.x.

Bhattacharya, B.S., Bond, T.P., O'Hare, L., Turner, D., Durrant, S.J., 2016. Causal role of thalamic interneurons in brain state transitions: a study using a neural mass model implementing synaptic kinetics. Front. Comput. Neurosci. 10 https://doi.org/10.3389/fncom.2016.00115.

Bista, P., Pawlowski, M., Cerina, M., Ehling, P., Leist, M., Meuth, P., Aissaoui, A., Borsotto, M., Heurteaux, C., Decher, N., Pape, H.-C., Oliver, D., Meuth, S.G., Budde, T., 2015. Differential phospholipase C-dependent modulation of TASK and TREK two-pore domain K+ channels in rat thalamocortical relay neurons. J. Physiol. 593, 127–144. https://doi.org/10.1113/jphysiol.2014.276527.

Blanchard, S., Saillet, S., Ivanov, A., Benquet, P., Bénar, C.-G., Pélégrini-Issac, M., Benali, H., Wendling, F., 2016. A new computational model for neuro-glio-Vascular coupling: astrocyte activation can explain cerebral blood flow nonlinear response to interictal events. PLoS One 11. https://doi.org/10.1371/journal.pone.0147292.

Blethyn, K.L., Hughes, S.W., Crunelli, V., 2008. Evidence for electrical synapses between neurons of the nucleus reticularis thalami in the adult brain in vitro. Thalamus Relat. Syst. 4, 13–20. https://doi.org/10.1017/S1472928807000325.

Blitz, D.M., Regehr, W.G., 2005. Timing and specificity of feed-forward inhibition within the LGN. Neuron 45, 917–928. https://doi.org/10.1016/j.neuron.2005.01.033.

Bokor, H., Frère, S.G.A., Eyre, M.D., Slézia, A., Ulbert, I., Lüthi, A., Acsády, L., 2005. Selective GABAergic control of higher-order thalamic relays. Neuron 45, 929–940. https://doi.org/10.1016/j.neuron.2005.01.048.

Bourassa, J., Deschenes, M., 1995. Corticothalamic projections from the primary visual cortex in rats: a single fiber study using biocytin as an anterograde tracer. Neuroscience 66, 253–263.
Bourassa, J., Pinault, D., Deschênes, M., 1995. Corticothalamic projections from the cortical barrel field to the somatosensory thalamus in rats: a single-fibre study using biocytin as an anterograde tracer. Eur. J. Neurosci. 7, 19–30.
Bradfield, L.A., Hart, G., Balleine, B.W., 2013. The role of the anterior, mediodorsal, and parafascicular thalamus in instrumental conditioning. Front. Syst. Neurosci. 7 https://doi.org/10.3389/fnsys.2013.00051.
Briggs, F., Usrey, W.M., 2007. A fast, reciprocal pathway between the lateral geniculate nucleus and visual cortex in the macaque monkey. J. Neurosci. 27, 5431–5436. https://doi.org/10.1523/JNEUROSCI.1035-07.2007.
Briggs, F., Usrey, W.M., 2008. Emerging views of corticothalamic function. Curr. Opin. Neurobiol. 18, 403–407. https://doi.org/10.1016/j.conb.2008.09.002.
Brodovskaya, A., Kapur, J., 2019. Circuits generating secondarily generalized seizures. Epilepsy Behav. 101, 106474 https://doi.org/10.1016/j.yebeh.2019.106474. Status Epilepticus.
Budde, T., Munsch, T., Pape, H.C., 1998. Distribution of L-type calcium channels in rat thalamic neurones. Eur. J. Neurosci. 10, 586–597.
Bureš, J., Burešová, O., Fifková, E., Rabending, G., 1965. Reversible deafferentation of cerebral cortex by thalamic spreading depression. Exp. Neurol. 12, 55–67. https://doi.org/10.1016/0014-4886(65)90098-1.
Butts, D.A., Weng, C., Jin, J., Alonso, J.-M., Paninski, L., 2011. Temporal precision in the visual pathway through the interplay of excitation and stimulus-driven suppression. J. Neurosci. 31, 11313–11327. https://doi.org/10.1523/JNEUROSCI.0434-11.2011.
Buzsaki, G., 2006. Rhythms of the Brain. Oxford University Press.
Cappe, C., Morel, A., Barone, P., Rouiller, E.M., 2009. The thalamocortical projection systems in primate: an anatomical support for multisensory and sensorimotor interplay. Cereb. Cortex N. Y. N 1991 19, 2025–2037. https://doi.org/10.1093/cercor/bhn228.
Casas-Torremocha, D., Porrero, C., Rodriguez-Moreno, J., García-Amado, M., Lübke, J.H. R., Núñez, Á., Clascá, F., 2019. Posterior thalamic nucleus axon terminals have different structure and functional impact in the motor and somatosensory vibrissal cortices. Brain Struct. Funct. 224, 1627–1645. https://doi.org/10.1007/s00429-019-01862-4.
Casti, A., Hayot, F., Xiao, Y., Kaplan, E., 2008. A simple model of retina-LGN transmission. J. Comput. Neurosci. 24, 235–252. https://doi.org/10.1007/s10827-007-0053-7.
Cavdar, S., Onat, F., Cakmak, Y.O., Saka, E., Yananli, H.R., Aker, R., 2006. Connections of the zona incerta to the reticular nucleus of the thalamus in the rat. J. Anat. 209, 251–258. https://doi.org/10.1111/j.1469-7580.2006.00600.x.
Cavdar, S., Bay, H.H., Kirazli, O., Cakmak, Y.O., Onat, F., 2013. Comparing GABAergic cell populations in the thalamic reticular nucleus of normal and genetic absence epilepsy rats from Strasbourg (GAERS). Neurol. Sci. Off. J. Ital. Neurol. Soc. Ital. Soc. Clin. Neurophysiol. 34, 1991–2000. https://doi.org/10.1007/s10072-013-1435-4.
Cavdar, S., Bay, H.H., Yildiz, S.D., Akakin, D., Sirvanci, S., Onat, F., 2014. Comparison of numbers of interneurons in three thalamic nuclei of normal and epileptic rats. Neurosci. Bull. 30, 451–460. https://doi.org/10.1007/s12264-013-1402-3.
Cerina, M., Szkudlarek, H.J., Coulon, P., Meuth, P., Kanyshkova, T., Nguyen, X.V., Göbel, K., Seidenbecher, T., Meuth, S.G., Pape, H.-C., Budde, T., 2015. Thalamic Kv 7 channels: pharmacological properties and activity control during noxious signal processing. Br. J. Pharmacol. 172, 3126–3140. https://doi.org/10.1111/bph.13113.
Chander, B.S., Chakravarthy, V.S., 2012. A computational model of neuro-glio-vascular loop interactions. PLoS One 7, e48802. https://doi.org/10.1371/journal.pone.0048802.
Chhabria, K., Chakravarthy, V.S., 2016. Low-dimensional models of "Neuro-Glio-Vascular unit" for describing neural dynamics under normal and energy-starved conditions. Front. Neurol. 7 https://doi.org/10.3389/fneur.2016.00024.
Cicirata, F., Angaut, P., Serapide, M.F., Panto, M.R., 1990. Functional organization of the direct and indirect projection via the reticularis thalami nuclear complex from the motor cortex to the thalamic nucleus ventralis lateralis. Exp. Brain Res. 79, 325–337. https://doi.org/10.1007/bf00608242.
Clasca, F., Rubio-Garrido, P., Jabaudon, D., 2012. Unveiling the diversity of thalamocortical neuron subtypes. Eur. J. Neurosci. 35, 1524–1532. https://doi.org/10.1111/j.1460-9568.2012.08033.x.
Clemente-Perez, A., Makinson, S.R., Higashikubo, B., Brovarney, S., Cho, F.S., Urry, A., Holden, S.S., Wimer, M., Dávid, C., Fenno, L.E., Acsády, L., Deisseroth, K., Paz, J.T., 2017. Distinct thalamic reticular cell types differentially modulate normal and pathological cortical rhythms. Cell Rep. 19, 2130–2142. https://doi.org/10.1016/j.celrep.2017.05.044.
Cone, A.C., Ambrosi, C., Scemes, E., Martone, M.E., Sosinsky, G., 2013. A comparative antibody analysis of Pannexin1 expression in four rat brain regions reveals varying subcellular localizations. Front. Pharmacol. 4 https://doi.org/10.3389/fphar.2013.00006.
Connelly, W.M., Crunelli, V., Errington, A.C., 2015. The global spike: conserved dendritic properties enable unique Ca2+ spike generation in low-threshold spiking neurons. J. Neurosci. Off. J. Soc. Neurosci. 35, 15505–15522. https://doi.org/10.1523/JNEUROSCI.2740-15.2015.
Connors, B.W., Long, M.A., 2004. Electrical synapses in the mammalian brain. Annu. Rev. Neurosci. 27, 393–418. https://doi.org/10.1146/annurev.neuro.26.041002.131128.
Copeland, C.S., Wall, T.M., Sims, R.E., Neale, S.A., Nisenbaum, E., Parri, H.R., Salt, T.E., 2017. Astrocytes modulate thalamic sensory processing via mGlu2 receptor activation. Neuropharmacology 121, 100–110. https://doi.org/10.1016/j.neuropharm.2017.04.019.
Cox, C.L., Beatty, J.A., 2017. The multifaceted role of inhibitory interneurons in the dorsal lateral geniculate nucleus. Vis. Neurosci. 34, E017. https://doi.org/10.1017/S0952523817000141.
Cox, C.L., Sherman, S.M., 2000. Control of dendritic outputs of inhibitory interneurons in the lateral geniculate nucleus. Neuron 27, 597–610. https://doi.org/10.1016/S0896-6273(00)00069-6.
Cox, C.L., Huguenard, J.R., Prince, D.A., 1997. Nucleus reticularis neurons mediate diverse inhibitory effects in thalamus. Proc. Natl. Acad. Sci. U. S. A. 94, 8854–8859.
Cox, C.L., Reichova, I., Sherman, S.M., 2003. Functional synaptic contacts by intranuclear axon collaterals of thalamic relay neurons. J. Neurosci. Off. J. Soc. Neurosci. 23, 7642–7646.
Crabtree, J.W., 1999. Intrathalamic sensory connections mediated by the thalamic reticular nucleus. Cell. Mol. Life Sci. CMLS 56, 683–700. https://doi.org/10.1007/s000180050462.
Crabtree, J.W., Collingridge, G.L., Isaac, J.T., 1998. A new intrathalamic pathway linking modality-related nuclei in the dorsal thalamus. Nat. Neurosci. 1, 389–394. https://doi.org/10.1038/1603.
Crandall, S.R., Cox, C.L., 2013. Thalamic microcircuits: presynaptic dendrites form two feedforward inhibitory pathways in thalamus. J. Neurophysiol. 110, 470–480. https://doi.org/10.1152/jn.00559.2012.
Crandall, S.R., Govindaiah, G., Cox, C.L., 2010. Low-threshold Ca2+ current amplifies distal dendritic signaling in thalamic reticular neurons. J. Neurosci. Off. J. Soc. Neurosci. 30, 15419–15429. https://doi.org/10.1523/JNEUROSCI.3636-10.2010.
Crandall, S.R., Cruikshank, S.J., Connors, B.W., 2015. A corticothalamic switch: controlling the thalamus with dynamic synapses. Neuron 86, 768–782. https://doi.org/10.1016/j.neuron.2015.03.040.
Cruikshank, S.J., Killackey, H.P., Metherate, R., 2001. Parvalbumin and calbindin are differentially distributed within primary and secondary subregions of the mouse auditory forebrain. Neuroscience 105, 553–569. https://doi.org/10.1016/s0306-4522(01)00226-3.
Cueni, L., Canepari, M., Luján, R., Emmenegger, Y., Watanabe, M., Bond, C.T., Franken, P., Adelman, J.P., Lüthi, A., 2008. T-type Ca2+ channels, SK2 channels and SERCAs gate sleep-related oscillations in thalamic dendrites. Nat. Neurosci. 11, 683–692. https://doi.org/10.1038/nn.2124.
Curró Dossi, R., Nuñez, A., Steriade, M., 1992. Electrophysiology of a slow (0.5-4 Hz) intrinsic oscillation of cat thalamocortical neurones in vivo. J. Physiol. 447, 215–234. https://doi.org/10.1113/jphysiol.1992.sp018999.
Datunashvili, M., Chaudhary, R., Zobeiri, M., Lüttjohann, A., Mergia, E., Baumann, A., Balfanz, S., Budde, B., van Luijtelaar, G., Pape, H.-C., Koesling, D., Budde, T., 2018. Modulation of hyperpolarization-activated inward current and thalamic activity modes by different cyclic nucleotides. Front. Cell. Neurosci. 12 https://doi.org/10.3389/fncel.2018.00369.
de Biasi, S., Frassoni, C., Spreafico, R., 1986. GABA immunoreactivity in the thalamic reticular nucleus of the rat. A light and electron microscopical study. Brain Res. 399, 143–147.
De Biasi, S., Arcelli, P., Spreafico, R., 1994. Parvalbumin immunoreactivity in the thalamus of guinea pig: light and electron microscopic correlation with gamma-aminobutyric acid immunoreactivity. J. Comp. Neurol. 348, 556–569. https://doi.org/10.1002/cne.903480406.
Deans, M.R., Gibson, J.R., Sellitto, C., Connors, B.W., Paul, D.L., 2001. Synchronous activity of inhibitory networks in neocortex requires electrical synapses containing connexin36. Neuron 31, 477–485. https://doi.org/10.1016/s0896-6273(01)00373-7.
Deisseroth, K., 2015. Optogenetics: 10 years of microbial opsins in neuroscience. Nat. Neurosci. 18, 1213–1225. https://doi.org/10.1038/nn.4091.
Deleuze, C., Huguenard, J.R., 2006. Distinct electrical and chemical connectivity maps in the thalamic reticular nucleus: potential roles in synchronization and sensation. J. Neurosci. Off. J. Soc. Neurosci. 26, 8633–8645. https://doi.org/10.1523/JNEUROSCI.2333-06.2006.
Deschênes, M., Bourassa, J., Pinault, D., 1994. Corticothalamic projections from layer V cells in rat are collaterals of long-range corticofugal axons. Brain Res. 664, 215–219.
Deschênes, M., Veinante, P., Zhang, Z.-W., 1998. The organization of corticothalamic projections: reciprocity versus parity. Brain Res. Rev. 28, 286–308. https://doi.org/10.1016/S0165-0173(98)00017-4.
Desilets-Roy, B., Varga, C., Lavallee, P., Deschenes, M., 2002. Substrate for cross-talk inhibition between thalamic barreloids. J. Neurosci. Off. J. Soc. Neurosci. 22, RC218 https://doi.org/20026338.
Diaz, F., Villena, A., Gonzalez, P., Requena, V., Rius, F., Perez De Vargas, I., 1999. Stereological age-related changes in neurons of the rat dorsal lateral geniculate nucleus. Anat. Rec. 255, 396–400. https://doi.org/10.1002/(SICI)1097-0185(19990801)255:4<396::AID-AR5>3.0.CO;2-M.
Ebner, F.F., Kaas, J.H., 2015. Chapter 24 - somatosensory system A2. In: Paxinos, G. (Ed.), The Rat Nervous System. Academic Press, San Diego, pp. 675–701.
Economo, M.N., Clack, N.G., Lavis, L.D., Gerfen, C.R., Svoboda, K., Myers, E.W., Chandrashekar, J., 2016. A platform for brain-wide imaging and reconstruction of individual neurons. eLife 5, e10566. https://doi.org/10.7554/eLife.10566.
Ehling, P., Cerina, M., Meuth, P., Kanyshkova, T., Bista, P., Coulon, P., Meuth, S.G., Pape, H.-C., Budde, T., 2013. Ca(2+)-dependent large conductance K(+) currents in thalamocortical relay neurons of different rat strains. Pflugers Arch. 465, 469–480. https://doi.org/10.1007/s00424-012-1188-6.
El-Boustani, S., Sermet, B.S., Foustoukos, G., Oram, T.B., Yizhar, O., Petersen, C.C.H., 2020. Anatomically and functionally distinct thalamocortical inputs to primary and secondary mouse whisker somatosensory cortices. Nat. Commun. 11, 3342. https://doi.org/10.1038/s41467-020-17087-7.

Emmers, R., 1965. Organization of the first and the second somesthetic regions (SI and SII) in the rat thalamus. J. Comp. Neurol. 124, 215–227. https://doi.org/10.1002/cne.901240207.
Erö, C., Gewaltig, M.-O., Keller, D., Markram, H., 2018. A cell atlas for the mouse brain. Front. Neuroinformatics 12. https://doi.org/10.3389/fninf.2018.00084.
Errington, A.C., Renger, J.J., Uebele, V.N., Crunelli, V., 2010. State-dependent firing determines intrinsic dendritic Ca2+ signaling in thalamocortical neurons. J. Neurosci. Off. J. Soc. Neurosci. 30, 14843–14853. https://doi.org/10.1523/JNEUROSCI.2968-10.2010.
Evangelio, M., García-Amado, M., Clascá, F., 2018. Thalamocortical projection neuron and interneuron numbers in the visual thalamic nuclei of the adult C57BL/6 mouse. Front. Neuroanat. 12 https://doi.org/10.3389/fnana.2018.00027.
Fabri, M., Burton, H., 1991. Topography of connections between primary somatosensory cortex and posterior complex in rat: a multiple fluorescent tracer study. Brain Res. 538, 351–357. https://doi.org/10.1016/0006-8993(91)90455-5.
Feldmeyer, D., 2012. Excitatory neuronal connectivity in the barrel cortex. Front. Neuroanat. 6 https://doi.org/10.3389/fnana.2012.00024.
Ferri, J., Ford, J.M., Roach, B.J., Turner, J.A., Erp, T.Gvan, Voyvodic, J., Preda, A., Belger, A., Bustillo, J., O'Leary, D., Mueller, B.A., Lim, K.O., McEwen, S.C., Calhoun, V.D., Diaz, M., Glover, G., Greve, D., Wible, C.G., Vaidya, J.G., Potkin, S.G., Mathalon, D.H., 2018. Resting-state thalamic dysconnectivity in schizophrenia and relationships with symptoms. Psychol. Med. 48, 2492–2499. https://doi.org/10.1017/S003329171800003X.
Fogerson, P.M., Huguenard, J.R., 2016. Tapping the brakes: cellular and synaptic mechanisms that regulate thalamic oscillations. Neuron 92, 687–704. https://doi.org/10.1016/j.neuron.2016.10.024.
Francis, J.T., Xu, S., Chapin, J.K., 2008. Proprioceptive and cutaneous representations in the rat ventral posterolateral thalamus. J. Neurophysiol. 99, 2291–2304. https://doi.org/10.1152/jn.01206.2007.
Frangeul, L., Porrero, C., Garcia-Amado, M., Maimone, B., Maniglier, M., Clascá, F., Jabaudon, D., 2014. Specific activation of the paralemniscal pathway during nociception. Eur. J. Neurosci. 39, 1455–1464. https://doi.org/10.1111/ejn.12524.
Funahashi, S., 2013. Thalamic mediodorsal nucleus and its participation in spatial working memory processes: comparison with the prefrontal cortex. Front. Syst. Neurosci. 7 https://doi.org/10.3389/fnsys.2013.00036.
Fürth, D., Vaissière, T., Tzortzi, O., Xuan, Y., Märtin, A., Lazaridis, I., Spigolon, G., Fisone, G., Tomer, R., Deisseroth, K., Carlén, M., Miller, C.A., Rumbaugh, G., Meletis, K., 2018. An interactive framework for whole-brain maps at cellular resolution. Nat. Neurosci. 21, 139–149. https://doi.org/10.1038/s41593-017-0027-7.
Gauriau, C., Bernard, J.-F., 2004. A comparative reappraisal of projections from the superficial laminae of the dorsal horn in the rat: the forebrain. J. Comp. Neurol. 468, 24–56. https://doi.org/10.1002/cne.10873.
Gentet, L.J., Ulrich, D., 2003. Strong, reliable and precise synaptic connections between thalamic relay cells and neurones of the nucleus reticularis in juvenile rats. J. Physiol. 546, 801–811.
Ghosh, K.K., Burns, L.D., Cocker, E.D., Nimmerjahn, A., Ziv, Y., Gamal, A.E., Schnitzer, M.J., 2011. Miniaturized integration of a fluorescence microscope. Nat. Methods 8, 871–878. https://doi.org/10.1038/nmeth.1694.
Giber, K., Slézia, A., Bokor, H., Bodor, A.L., Ludányi, A., Katona, I., Acsády, L., 2008. Heterogeneous output pathways link the anterior pretectal nucleus with the zona incerta and the thalamus in rat. J. Comp. Neurol. 506, 122–140. https://doi.org/10.1002/cne.21545.
Giesler, G.J., Björkeland, M., Xu, Q., Grant, G., 1988. Organization of the spinocervicothalamic pathway in the rat. J. Comp. Neurol. 268, 223–233. https://doi.org/10.1002/cne.902680207.
Gilbert, C.D., Wiesel, T.N., 1979. Morphology and intracortical projections of functionally characterised neurones in the cat visual cortex. Nature 280, 120–125. https://doi.org/10.1038/280120a0.
Golshani, P., Liu, X.-B., Jones, E.G., 2001. Differences in quantal amplitude reflect GluR4- subunit number at corticothalamic synapses on two populations of thalamic neurons. Proc. Natl. Acad. Sci. U. S. A. 98, 4172–4177. https://doi.org/10.1073/pnas.061013698.
Gong, H., Xu, D., Yuan, J., Li, X., Guo, C., Peng, J., Li, Y., Schwarz, L.A., Li, A., Hu, B., Xiong, B., Sun, Q., Zhang, Y., Liu, J., Zhong, Q., Xu, T., Zeng, S., Luo, Q., 2016. High-throughput dual-colour precision imaging for brain-wide connectome with cytoarchitectonic landmarks at the cellular level. Nat. Commun. 7, 12142. https://doi.org/10.1038/ncomms12142.
Gonzalo-Ruiz, A., Lieberman, A.R., 1995a. Topographic organization of projections from the thalamic reticular nucleus to the anterior thalamic nuclei in the rat. Brain Res. Bull. 37, 17–35.
Gonzalo-Ruiz, A., Lieberman, A.R., 1995b. GABAergic projections from the thalamic reticular nucleus to the anteroventral and anterodorsal thalamic nuclei of the rat. J. Chem. Neuroanat. 9, 165–174.
Graziano, A., Liu, X.-B., Murray, K.D., Jones, E.G., 2008. Vesicular glutamate transporters define two sets of glutamatergic afferents to the somatosensory thalamus and two thalamocortical projections in the mouse. J. Comp. Neurol. 507, 1258–1276. https://doi.org/10.1002/cne.21592.
Groh, A., Bokor, H., Mease, R.A., Plattner, V.M., Hangya, B., Stroh, A., Deschenes, M., Acsády, L., 2014. Convergence of cortical and sensory driver inputs on single thalamocortical cells. Cereb. Cortex N. Y. N 1991 (24), 3167–3179. https://doi.org/10.1093/cercor/bht173.
Guillery, R.W., Harting, J.K., 2003. Structure and connections of the thalamic reticular nucleus: advancing views over half a century. J. Comp. Neurol. 463, 360–371. https://doi.org/10.1002/cne.10738.
Guillery, R.W., Sherman, S.M., 2002. Thalamic relay functions and their role in corticocortical communication: generalizations from the visual system. Neuron 33, 163–175. https://doi.org/10.1016/S0896-6273(01)00582-7.
Gymnopoulos, M., Cingolani, L.A., Pedarzani, P., Stocker, M., 2014. Developmental mapping of small-conductance calcium-activated potassium channel expression in the rat nervous system. J. Comp. Neurol. 522, 1072–1101. https://doi.org/10.1002/cne.23466.
Haas, J.S., Zavala, B., Landisman, C.E., 2011. Activity-dependent long-term depression of electrical synapses. Science 334, 389–393. https://doi.org/10.1126/science.1207502.
Haidarliu, S., Ahissar, E., 2001. Size gradients of barreloids in the rat thalamus. J. Comp. Neurol. 429, 372–387.
Haidarliu, S., Yu, C., Rubin, N., Ahissar, E., 2008. Lemniscal and extralemniscal compartments in the VPM of the rat. Front. Neuroanat. 2, 4. https://doi.org/10.3389/neuro.05.004.2008.
Halassa, M.M., Acsády, L., 2016. Thalamic inhibition: diverse sources, diverse scales. Trends Neurosci. 39, 680–693. https://doi.org/10.1016/j.tins.2016.08.001.
Halász, P., 2013. How sleep activates epileptic networks? Epilepsy Res. Treat. 2013 https://doi.org/10.1155/2013/425697.
Hale, P.T., Sefton, A.J., Baur, L.A., Cottee, L.J., 1982. Interrelations of the rat's thalamic reticular and dorsal lateral geniculate nuclei. Exp. Brain Res. 45, 217–229.
Hamos, J.E., Van Horn, S.C., Raczkowski, D., Uhlrich, D.J., Sherman, S.M., 1985. Synaptic connectivity of a local circuit neurone in lateral geniculate nucleus of the cat. Nature 317, 618–621. https://doi.org/10.1038/317618a0.
Harris, R.M., 1986. Morphology of physiologically identified thalamocortical relay neurons in the rat ventrobasal thalamus. J. Comp. Neurol. 251, 491–505. https://doi.org/10.1002/cne.902510405.
Harris, R.M., 1987. Axon collaterals in the thalamic reticular nucleus from thalamocortical neurons of the rat ventrobasal thalamus. J. Comp. Neurol. 258, 397–406. https://doi.org/10.1002/cne.902580308.
Harris, R.M., Hendrickson, A.E., 1987. Local circuit neurons in the rat ventrobasal thalamus–a GABA immunocytochemical study. Neuroscience 21, 229–236. https://doi.org/10.1016/0306-4522(87)90335-6.
Hayama, T., Hashimoto, K., Ogawa, H., 1994. Anatomical location of a taste-related region in the thalamic reticular nucleus in rats. Neurosci. Res. 18, 291–299.
Heiberg, T., Hagen, E., Halnes, G., Einevoll, G.T., 2016. Biophysical network modelling of the dLGN circuit: different effects of triadic and axonal inhibition on visual responses of relay cells. PLoS Comput. Biol. 12, e1004929 https://doi.org/10.1371/journal.pcbi.1004929.
Hill, S.L., Tononi, G., 2005. Modeling sleep and wakefulness in the thalamocortical system. J. Neurophysiol. 93, 1671–1698. https://doi.org/10.1152/jn.00915.2004.
Hill, S.L., Wang, Y., Riachi, I., Schürmann, F., Markram, H., 2012. Statistical connectivity provides a sufficient foundation for specific functional connectivity in neocortical neural microcircuits. Proc. Natl. Acad. Sci. 109, E2885–E2894. https://doi.org/10.1073/pnas.1202128109.
Hoerder-Suabedissen, A., Hayashi, S., Upton, L., Nolan, Z., Casas-Torremocha, D., Grant, E., Viswanathan, S., Kanold, P.O., Clasca, F., Kim, Y., Molnár, Z., 2018. Subset of cortical layer 6b neurons selectively innervates higher order thalamic nuclei in mice. Cereb. Cortex N. Y. N 1991 (28), 1882–1897. https://doi.org/10.1093/cercor/bhy036.
Hoogland, P.V., Welker, E., Van der Loos, H., 1987. Organization of the projections from barrel cortex to thalamus in mice studied with Phaseolus vulgaris-leucoagglutinin and HRP. Exp. Brain Res. 68, 73–87. https://doi.org/10.1007/bf00255235.
Hoogland, P.V., Wouterlood, F.G., Welker, E., Van der Loos, H., 1991. Ultrastructure of giant and small thalamic terminals of cortical origin: a study of the projections from the barrel cortex in mice using Phaseolus vulgaris leuco-agglutinin (PHA-L). Exp. Brain Res. 87, 159–172. https://doi.org/10.1007/BF00228517.
Hou, G., Smith, A.G., Zhang, Z.-W., 2016. Lack of intrinsic GABAergic connections in the thalamic reticular nucleus of the mouse. J. Neurosci. 36, 7246–7252. https://doi.org/10.1523/JNEUROSCI.0607-16.2016.
Huang, Y., Grinspan, J.B., Abrams, C.K., Scherer, S.S., 2007. Pannexin1 is expressed by neurons and glia but does not form functional gap junctions. Glia 55, 46–56. https://doi.org/10.1002/glia.20435.
Hughes, S.W., Cope, D.W., Blethyn, K.L., Crunelli, V., 2002. Cellular mechanisms of the slow (<1 Hz) oscillation in thalamocortical neurons in vitro. Neuron 33, 947–958. https://doi.org/10.1016/s0896-6273(02)00623-2.
Huguenard, J.R., Prince, D.A., 1991. Slow inactivation of a TEA-sensitive K current in acutely isolated rat thalamic relay neurons. J. Neurophysiol. 66, 1316–1328. https://doi.org/10.1152/jn.1991.66.4.1316.
Huguenard, J.R., Prince, D.A., 1994. Intrathalamic rhythmicity studied in vitro: nominal T-current modulation causes robust antioscillatory effects. J. Neurosci. Off. J. Soc. Neurosci. 14, 5485–5502.
Huntsman, M.M., Porcello, D.M., Homanics, G.E., DeLorey, T.M., Huguenard, J.R., 1999. Reciprocal inhibitory connections and network synchrony in the mammalian thalamus. Science 283, 541–543. https://doi.org/10.1126/science.283.5401.541.
Huusko, N., Pitkanen, A., 2014. Parvalbumin immunoreactivity and expression of GABAA receptor subunits in the thalamus after experimental TBI. Neuroscience 267, 30–45. https://doi.org/10.1016/j.neuroscience.2014.02.026.
Iavarone, E., Yi, J., Shi, Y., Zandt, B.-J., O'Reilly, C., Geit, W.V., Rössert, C., Markram, H., Hill, S.L., 2019. Experimentally-constrained biophysical models of tonic and burst firing modes in thalamocortical neurons. PLoS Comput. Biol. 15, e1006753 https://doi.org/10.1371/journal.pcbi.1006753.
Iidaka, T., Kogata, T., Mano, Y., Komeda, H., 2019. Thalamocortical hyperconnectivity and amygdala-cortical hypoconnectivity in male patients with autism spectrum disorder. Front. Psychiatry 10. https://doi.org/10.3389/fpsyt.2019.00252.

Imam, F.T., Larson, S.D., Bandrowski, A., Grethe, J.S., Gupta, A., Martone, M.E., 2012. Development and use of ontologies inside the neuroscience information framework: a practical approach. Front. Genet. 3 https://doi.org/10.3389/fgene.2012.00111.
Izhikevich, E.M., Edelman, G.M., 2008. Large-scale model of mammalian thalamocortical systems. Proc. Natl. Acad. Sci. 105, 3593–3598. https://doi.org/10.1073/pnas.0712231105.
Jager, P., Ye, Z., Yu, X., Zagoraiou, L., Prekop, H.-T., Partanen, J., Jessell, T.M., Wisden, W., Brickley, S.G., Delogu, A., 2016. Tectal-derived interneurons contribute to phasic and tonic inhibition in the visual thalamus. Nat. Commun. 7, 13579. https://doi.org/10.1038/ncomms13579.
Jager, P., Moore, G., Calpin, P., Durmishi, X., Salgarella, I., Menage, L., Kita, Y., Wang, Y., Kim, D.W., Blackshaw, S., Schultz, S.R., Brickley, S., Shimogori, T., Delogu, A., 2021. Dual midbrain and forebrain origins of thalamic inhibitory interneurons. eLife 10, e59272. https://doi.org/10.7554/eLife.59272.
Jahnsen, H., Llinas, R., 1984. Electrophysiological properties of guinea-pig thalamic neurones: an in vitro study. J. Physiol. 349, 205–226.
Jankowski, M.M., Ronnqvist, K.C., Tsanov, M., Vann, S.D., Wright, N.F., Erichsen, J.T., Aggleton, J.P., O'Mara, S.M., 2013. The anterior thalamus provides a subcortical circuit supporting memory and spatial navigation. Front. Syst. Neurosci. 7 https://doi.org/10.3389/fnsys.2013.00045.
Ji, X., Zingg, B., Mesik, L., Xiao, Z., Zhang, L.I., Tao, H.W., 2016. Thalamocortical innervation pattern in mouse auditory and visual cortex: laminar and cell-type specificity. Cereb. Cortex 26, 2612–2625. https://doi.org/10.1093/cercor/bhv099.
Jones, E.G., 1975. Some aspects of the organization of the thalamic reticular complex. J. Comp. Neurol. 162, 285–308. https://doi.org/10.1002/cne.901620302.
Jones, E.G., 2002. Thalamic organization and function after Cajal. Prog. Brain Res. 136, 333–357.
Jones, E.G., 2007. The Thalamus, 2nd ed. Cambridge University Press, Cambridge, Cambridge.
Jones, E.G., Hendry, S.H.C., 1989. Differential calcium binding protein immunoreactivity distinguishes classes of relay neurons in monkey thalamic nuclei. Eur. J. Neurosci. 1, 222–246. https://doi.org/10.1111/j.1460-9568.1989.tb00791.x.
Jun, J.J., Steinmetz, N.A., Siegle, J.H., Denman, D.J., Bauza, M., Barbarits, B., Lee, A.K., Anastassiou, C.A., Andrei, A., Aydın, Ç., Barbic, M., Blanche, T.J., Bonin, V., Couto, J., Dutta, B., Gratiy, S.L., Gutnisky, D.A., Häusser, M., Karsh, B., Ledochowitsch, P., Lopez, C.M., Mitelut, C., Musa, S., Okun, M., Pachitariu, M., Putzeys, J., Rich, P.D., Rossant, C., Sun, W., Svoboda, K., Carandini, M., Harris, K.D., Koch, C., O'Keefe, J., Harris, T.D., 2017. Fully integrated silicon probes for high-density recording of neural activity. Nature 551, 232–236. https://doi.org/10.1038/nature24636.
Kanyshkova, T., Pawlowski, M., Meuth, P., Dubé, C., Bender, R.A., Brewster, A.L., Baumann, A., Baram, T.Z., Pape, H.-C., Budde, T., 2009. Postnatal expression pattern of HCN channel isoforms in thalamic neurons: relationship to maturation of thalamocortical oscillations. J. Neurosci. Off. J. Soc. Neurosci. 29, 8847–8857. https://doi.org/10.1523/JNEUROSCI.0689-09.2009.
Kanyshkova, T., Broicher, T., Meuth, S.G., Pape, H.-C., Budde, T., 2011. A-type K+ currents in intralaminar thalamocortical relay neurons. Pflugers Arch. 461, 545–556. https://doi.org/10.1007/s00424-011-0953-2.
Keller, D., Erö, C., Markram, H., 2018. Cell densities in the mouse brain: a systematic review. Front. Neuroanat. 12 https://doi.org/10.3389/fnana.2018.00083.
Kelly, M.K., Carvell, G.E., Hartings, J.A., Simons, D.J., 2001. Axonal conduction properties of antidromically identified neurons in rat barrel cortex. Somatosens. Mot. Res. 18, 202–210.
Kerschensteiner, D., Guido, W., 2017. Organization of the dorsal lateral geniculate nucleus in the mouse. Vis. Neurosci. 34, E008. https://doi.org/10.1017/S0952523817000062.
Kim, U., McCormick, D.A., 1998. Functional and ionic properties of a slow afterhyperpolarization in ferret perigeniculate neurons in vitro. J. Neurophysiol. 80, 1222–1235. https://doi.org/10.1152/jn.1998.80.3.1222.
Kim, Y., Yang, G.R., Pradhan, K., Venkataraju, K.U., Bota, M., García Del Molino, L.C., Fitzgerald, G., Ram, K., He, M., Levine, J.M., Mitra, P., Huang, Z.J., Wang, X.-J., Osten, P., 2017. Brain-wide maps reveal stereotyped cell-type-Based cortical architecture and subcortical sexual dimorphism. Cell 171, 456–469. https://doi.org/10.1016/j.cell.2017.09.020 e22.
Kimura, A., Imbe, H., Donishi, T., Tamai, Y., 2007. Axonal projections of single auditory neurons in the thalamic reticular nucleus: implications for tonotopy-related gating function and cross-modal modulation. Eur. J. Neurosci. 26, 3524–3535. https://doi.org/10.1111/j.1460-9568.2007.05925.x.
Kimura, A., Yokoi, I., Imbe, H., Donishi, T., Kaneoke, Y., 2012. Auditory thalamic reticular nucleus of the rat: anatomical nodes for modulation of auditory and cross-modal sensory processing in the loop connectivity between the cortex and thalamus. J. Comp. Neurol. 520, 1457–1480. https://doi.org/10.1002/cne.22805.
Kinomura, S., Larsson, J., Gulyás, B., Roland, P.E., 1996. Activation by attention of the human reticular formation and thalamic intralaminar nuclei. Science 271, 512–515. https://doi.org/10.1126/science.271.5248.512.
Klingner, C.M., Langbein, K., Dietzek, M., Smesny, S., Witte, O.W., Sauer, H., Nenadic, I., 2014. Thalamocortical connectivity during resting state in schizophrenia. Eur. Arch. Psychiatry Clin. Neurosci. 264, 111–119. https://doi.org/10.1007/s00406-013-0417-0.
Klostermann, F., 2013. Functional roles of the thalamus for language capacities. Front. Syst. Neurosci. 7 https://doi.org/10.3389/fnsys.2013.00032.
Komura, Y., Tamura, R., Uwano, T., Nishijo, H., Kaga, K., Ono, T., 2001. Retrospective and prospective coding for predicted reward in the sensory thalamus. Nature 412, 546–549. https://doi.org/10.1038/35087595.
Koós, T., Tepper, J.M., 1999. Inhibitory control of neostriatal projection neurons by GABAergic interneurons. Nat. Neurosci. 2, 467–472. https://doi.org/10.1038/8138.
Krahe, T.E., El-Danaf, R.N., Dilger, E.K., Henderson, S.C., Guido, W., 2011. Morphologically distinct classes of relay cells exhibit regional preferences in the dorsal lateral geniculate nucleus of the mouse. J. Neurosci. 31, 17437–17448. https://doi.org/10.1523/JNEUROSCI.4370-11.2011.
Kwegyir-Afful, E.E., Simons, D.J., 2009. Subthreshold receptive field properties distinguish different classes of corticothalamic neurons in the somatosensory system. J. Neurosci. 29, 964–972. https://doi.org/10.1523/JNEUROSCI.3924-08.2009.
Lam, Y.-W., Sherman, S.M., 2005. Mapping by laser photostimulation of connections between the thalamic reticular and ventral posterior lateral nuclei in the rat. J. Neurophysiol. 94, 2472–2483. https://doi.org/10.1152/jn.00206.2005.
Lam, Y.-W., Sherman, S.M., 2010. Functional organization of the somatosensory cortical layer 6 feedback to the thalamus. Cereb. Cortex N. Y. N 1991 (20), 13–24. https://doi.org/10.1093/cercor/bhp077.
Lam, Y.-W., Sherman, S.M., 2011. Functional organization of the thalamic input to the thalamic reticular nucleus. J. Neurosci. Off. J. Soc. Neurosci. 31, 6791–6799. https://doi.org/10.1523/JNEUROSCI.3073-10.2011.
Lam, Y.-W., Nelson, C.S., Sherman, S.M., 2006. Mapping of the functional interconnections between thalamic reticular neurons using photostimulation. J. Neurophysiol. 96, 2593–2600. https://doi.org/10.1152/jn.00555.2006.
Landisman, C.E., Connors, B.W., 2005. Long-term modulation of electrical synapses in the mammalian thalamus. Science 310, 1809–1813. https://doi.org/10.1126/science.1114655.
Landisman, C.E., Long, M.A., Beierlein, M., Deans, M.R., Paul, D.L., Connors, B.W., 2002. Electrical synapses in the thalamic reticular nucleus. J. Neurosci. Off. J. Soc. Neurosci. 22, 1002–1009.
Lavallée, P., Urbain, N., Dufresne, C., Bokor, H., Acsády, L., Deschênes, M., 2005. Feedforward inhibitory control of sensory information in higher-order thalamic nuclei. J. Neurosci. Off. J. Soc. Neurosci. 25, 7489–7498. https://doi.org/10.1523/JNEUROSCI.2301-05.2005.
Lee, C.C., Sherman, S.M., 2010. Topography and physiology of ascending streams in the auditory tectothalamic pathway. Proc. Natl. Acad. Sci. U. S. A. 107, 372–377. https://doi.org/10.1073/pnas.0907873107.
Lee, S.-H., Govindaiah, G., Cox, C.L., 2007. Heterogeneity of firing properties among rat thalamic reticular nucleus neurons. J. Physiol. 582, 195–208. https://doi.org/10.1113/jphysiol.2007.134254.
Lee, S.-C., Cruikshank, S.J., Connors, B.W., 2010. Electrical and chemical synapses between relay neurons in developing thalamus. J. Physiol. 588, 2403–2415. https://doi.org/10.1113/jphysiol.2010.187096.
Lee, S.-C., Patrick, S.L., Richardson, K.A., Connors, B.W., 2014. Two functionally distinct networks of gap junction-coupled inhibitory neurons in the thalamic reticular nucleus. J. Neurosci. Off. J. Soc. Neurosci. 34, 13170–13182. https://doi.org/10.1523/JNEUROSCI.0562-14.2014.
Leist, M., Datunashvilli, M., Kanyshkova, T., Zobeiri, M., Aissaoui, A., Cerina, M., Romanelli, M.N., Pape, H.-C., Budde, T., 2016. Two types of interneurons in the mouse lateral geniculate nucleus are characterized by different h-current density. Sci. Rep. 6, 24904. https://doi.org/10.1038/srep24904.
Leresche, N., Asprodini, E., Emri, Z., Cope, D.W., Crunelli, V., 2000. Somatostatin inhibits GABAergic transmission in the sensory thalamus via presynaptic receptors. Neuroscience 98, 513–522.
LeVay, S., Ferster, D., 1979. Proportion of interneurons in the cat's lateral geniculate nucleus. Brain Res. 164, 304–308. https://doi.org/10.1016/0006-8993(79)90026-x.
Li, J., Bickford, M.E., Guido, W., 2003. Distinct firing properties of higher order thalamic relay neurons. J. Neurophysiol. 90, 291–299. https://doi.org/10.1152/jn.01163.2002.
Liao, C.-C., Chen, R.-F., Lai, W.-S., Lin, R.C.S., Yen, C.-T., 2010. Distribution of large terminal inputs from the primary and secondary somatosensory cortices to the dorsal thalamus in the rodent. J. Comp. Neurol. 518, 2592–2611. https://doi.org/10.1002/cne.22354.
Lifshitz, J., Kelley, B.J., Povlishock, J.T., 2007. Perisomatic thalamic axotomy after diffuse traumatic brain injury is associated with atrophy rather than cell death. J. Neuropathol. Exp. Neurol. 66, 218–229. https://doi.org/10.1097/01.jnen.0000248558.75950.4d.
Ling, C., Hendrickson, M.L., Kalil, R.E., 2012. Morphology, classification, and distribution of the projection neurons in the dorsal lateral geniculate nucleus of the rat. PLoS One 7, e49161. https://doi.org/10.1371/journal.pone.0049161.
Linke, A.C., Jao Keehn, R.J., Pueschel, E.B., Fishman, I., Müller, R.-A., 2018. Children with ASD show links between aberrant sound processing, social symptoms, and atypical auditory interhemispheric and thalamocortical functional connectivity. Dev. Cogn. Neurosci. 29, 117–126. https://doi.org/10.1016/j.dcn.2017.01.007. Autism Spectrum Condition – understanding sensory and social features.
Lintas, A., Schwaller, B., Villa, A.E.P., 2013. Visual thalamocortical circuits in parvalbumin-deficient mice. Brain Res. 1536, 107–118. https://doi.org/10.1016/j.brainres.2013.04.048.
Liu, X.-B., Jones, E.G., 1999. Predominance of corticothalamic synaptic inputs to thalamic reticular nucleus neurons in the rat. J. Comp. Neurol. 414, 67–79.
Liu, X.-B., Jones, E.G., 2003. Fine structural localization of connexin-36 immunoreactivity in mouse cerebral cortex and thalamus. J. Comp. Neurol. 466, 457–467. https://doi.org/10.1002/cne.10901.
Liu, C., Foffani, G., Scaglione, A., Aguilar, J., Moxon, K.A., 2017. Adaptation of thalamic neurons provides information about the spatiotemporal context of stimulus history. J. Neurosci. 37, 10012–10021. https://doi.org/10.1523/JNEUROSCI.0637-17.2017.
Lo, F.S., Sherman, S.M., 1994. Feedback inhibition in the cat's lateral geniculate nucleus. Exp. Brain Res. 100, 365–368. https://doi.org/10.1007/bf00227207.
Long, M.A., Landisman, C.E., Connors, B.W., 2004. Small clusters of electrically coupled neurons generate synchronous rhythms in the thalamic reticular nucleus.

J. Neurosci. Off. J. Soc. Neurosci. 24, 341–349. https://doi.org/10.1523/JNEUROSCI.3358-03.2004.
Lozsadi, D.A., 1994. Organization of cortical afferents to the rostral, limbic sector of the rat thalamic reticular nucleus. J. Comp. Neurol. 341, 520–533. https://doi.org/10.1002/cne.903410408.
Lozsadi, D.A., 1995. Organization of connections between the thalamic reticular and the anterior thalamic nuclei in the rat. J. Comp. Neurol. 358, 233–246. https://doi.org/10.1002/cne.903580206.
Lu, E., Llano, D.A., Sherman, S.M., 2009. Different distributions of calbindin and calretinin immunostaining across the medial and dorsal divisions of the mouse medial geniculate body. Hear. Res. 257, 16–23. https://doi.org/10.1016/j.heares.2009.07.009.
Lubke, J., 1993. Morphology of neurons in the thalamic reticular nucleus (TRN) of mammals as revealed by intracellular injections into fixed brain slices. J. Comp. Neurol. 329, 458–471. https://doi.org/10.1002/cne.903290404.
Luczynska, A., Dziewiatkowski, J., Jagalska-Majewska, H., Kowianski, P., Wojcik, S., Labuda, C., Morys, J., 2003. Qualitative and quantitative analysis of the postnatal development of the ventroposterolateral nucleus of the thalamus in rat and rabbit. Folia Morphol. 62, 75–87.
Luth, H.J., Winkelmann, E., Celio, M.R., 1993. Light- and electron microscopic localization of parvalbumin, calbindin D-28k and calretinin in the dorsal lateral geniculate nucleus of the rat. J. Hirnforsch. 34, 47–56.
Lüthi, A., 2014. Sleep spindles where they come from, what they do. Neuroscientist 20, 243–256. https://doi.org/10.1177/1073858413500854.
Majka, P., Kublik, E., Furga, G., Wójcik, D.K., 2012. Common atlas format and 3D brain atlas reconstructor: infrastructure for constructing 3D brain atlases. Neuroinformatics 10, 181–197. https://doi.org/10.1007/s12021-011-9138-6.
Makinson, C.D., Tanaka, B.S., Sorokin, J.M., Wong, J.C., Christian, C.A., Goldin, A.L., Escayg, A., Huguenard, J.R., 2017. Regulation of thalamic and cortical network synchrony by Scn8a. Neuron 93, 1165–1179. https://doi.org/10.1016/j.neuron.2017.01.031 e6.
Markram, H., 2006. The blue brain project. Nat. Rev. Neurosci. 7, 153–160. https://doi.org/10.1038/nrn1848.
Markram, H., Muller, E., Ramaswamy, S., Reimann, M.W., Abdellah, M., Sanchez, C.A., Ailamaki, A., Alonso-Nanclares, L., Antille, N., Arsever, S., Kahou, G.A.A., Berger, T. K., Bilgili, A., Buncic, N., Chalimourda, A., Chindemi, G., Courcol, J.-D., Delalondre, F., Delattre, V., Druckmann, S., Dumusc, R., Dynes, J., Eilemann, S., Gal, E., Gevaert, M.E., Ghobril, J.-P., Gidon, A., Graham, J.W., Gupta, A., Haenel, V., Hay, E., Heinis, T., Hernando, J.B., Hines, M., Kanari, L., Keller, D., Kenyon, J., Khazen, G., Kim, Y., King, J.G., Kisvarday, Z., Kumbhar, P., Lasserre, S., Le Bé, J.-V., Magalhães, B.R.C., Merchán-Pérez, A., Meystre, J., Morrice, B.R., Muller, J., Muñoz-Céspedes, A., Muralidhar, S., Muthurasa, K., Nachbaur, D., Newton, T.H., Nolte, M., Ovcharenko, A., Palacios, J., Pastor, L., Perin, R., Ranjan, R., Riachi, I., Rodríguez, J.-R., Riquelme, J.L., Rössert, C., Sfyrakis, K., Shi, Y., Shillcock, J.C., Silberberg, G., Silva, R., Tauheed, F., Telefont, M., Toledo-Rodriguez, M., Tränkler, T., Van Geit, W., Díaz, J.V., Walker, R., Wang, Y., Zaninetta, S.M., DeFelipe, J., Hill, S.L., Segev, I., Schürmann, F., 2015. Reconstruction and simulation of neocortical microcircuitry. Cell 163, 456–492. https://doi.org/10.1016/j.cell.2015.09.029.
McAllister, J.P., Wells, J., 1981. The structural organization of the ventral posterolateral nucleus in the rat. J. Comp. Neurol. 197, 271–301. https://doi.org/10.1002/cne.901970208.
McCormick, D.A., Bal, T., 1997. Sleep and arousal: thalamocortical mechanisms. Annu. Rev. Neurosci. 20, 185–215. https://doi.org/10.1146/annurev.neuro.20.1.185.
McCormick, D.A., Feeser, H.R., 1990. Functional implications of burst firing and single spike activity in lateral geniculate relay neurons. Neuroscience 39, 103–113. https://doi.org/10.1016/0306-4522(90)90225-s.
McCormick, D.A., Pape, H.C., 1990. Properties of a hyperpolarization-activated cation current and its role in rhythmic oscillation in thalamic relay neurones. J. Physiol. 431, 291–318.
Meuth, S.G., Kanyshkova, T., Meuth, P., Landgraf, P., Munsch, T., Ludwig, A., Hofmann, F., Pape, H.-C., Budde, T., 2006. Membrane resting potential of thalamocortical relay neurons is shaped by the interaction among TASK3 and HCN2 channels. J. Neurophysiol. 96, 1517–1529. https://doi.org/10.1152/jn.01212.2005.
Meyer, H.S., Wimmer, V.C., Hemberger, M., Bruno, R.M., de Kock, C.P.J., Frick, A., Sakmann, B., Helmstaedter, M., 2010. Cell type-specific thalamic innervation in a column of rat vibrissal cortex. Cereb. Cortex N. Y. N 1991 (20), 2287–2303. https://doi.org/10.1093/cercor/bhq069.
Meyer, H.S., Egger, R., Guest, J.M., Foerster, R., Reissl, S., Oberlaender, M., 2013. Cellular organization of cortical barrel columns is whisker-specific. Proc. Natl. Acad. Sci. 110, 19113–19118. https://doi.org/10.1073/pnas.1312691110.
Miller, R., 1996. Cortico-thalamic interplay and the security of operation of neural assemblies and temporal chains in the cerebral cortex. Biol. Cybern. 75, 263–275. https://doi.org/10.1007/s004220050293.
Mitrofanis, J., Guillery, R.W., 1993. New views of the thalamic reticular nucleus in the adult and the developing brain. Trends Neurosci. 16, 240–245. https://doi.org/10.1016/0166-2236(93)90163-G.
Mitrofanis, J., Mikuletic, L., 1999. Organisation of the cortical projection to the zona incerta of the thalamus. J. Comp. Neurol. 412, 173–185.
Mo, C., Petrof, I., Viaene, A.N., Sherman, S.M., 2017. Synaptic properties of the lemniscal and paralemniscal pathways to the mouse somatosensory thalamus. Proc. Natl. Acad. Sci. U. S. A. 114, E6212–E6221. https://doi.org/10.1073/pnas.1703222114.
Monavarfeshani, A., Sabbagh, U., Fox, M.A., 2017. Not a one-trick pony: diverse connectivity and functions of the rodent lateral geniculate complex. Vis. Neurosci. 34, E012. https://doi.org/10.1017/S0952523817000098.
Mooney, S.M., Miller, M.W., 2007. Postnatal generation of neurons in the ventrobasal nucleus of the rat thalamus. J. Neurosci. Off. J. Soc. Neurosci. 27, 5023–5032. https://doi.org/10.1523/JNEUROSCI.1194-07.2007.
Mooney, S.M., Miller, M.W., 2010. Prenatal exposure to ethanol affects postnatal neurogenesis in thalamus. Exp. Neurol. 223, 566–573. https://doi.org/10.1016/j.expneurol.2010.02.003.
Morgan, J.L., Lichtman, J.W., 2020. An individual interneuron participates in many kinds of inhibition and innervates much of the mouse visual thalamus. Neuron 106, 468–481. https://doi.org/10.1016/j.neuron.2020.02.001 e2.
Murakami, T.C., Mano, T., Saikawa, S., Horiguchi, S.A., Shigeta, D., Baba, K., Sekiya, H., Shimizu, Y., Tanaka, K.F., Kiyonari, H., Iino, M., Mochizuki, H., Tainaka, K., Ueda, H.R., 2018. A three-dimensional single-cell-resolution whole-brain atlas using CUBIC-X expansion microscopy and tissue clearing. Nat. Neurosci. 21, 625–637. https://doi.org/10.1038/s41593-018-0109-1.
Murray, J.D., Anticevic, A., 2017. Toward understanding thalamocortical dysfunction in schizophrenia through computational models of neural circuit dynamics. Schizophr. Res. 180, 70–77. https://doi.org/10.1016/j.schres.2016.10.021.
Nair, A., Treiber, J.M., Shukla, D.K., Shih, P., Müller, R.-A., 2013. Impaired thalamocortical connectivity in autism spectrum disorder: a study of functional and anatomical connectivity. Brain J. Neurol. 136, 1942–1955. https://doi.org/10.1093/brain/awt079.
Nakagawa, Y., 2019. Development of the thalamus: from early patterning to regulation of cortical functions. WIREs Dev. Biol. 8, e345. https://doi.org/10.1002/wdev.345.
Nothias, F., Peschanski, M., Besson, J.M., 1988. Somatotopic reciprocal connections between the somatosensory cortex and the thalamic Po nucleus in the rat. Brain Res. 447, 169–174. https://doi.org/10.1016/0006-8993(88)90980-8.
Notomi, T., Shigemoto, R., 2004. Immunohistochemical localization of Ih channel subunits, HCN1-4, in the rat brain. J. Comp. Neurol. 471, 241–276. https://doi.org/10.1002/cne.11039.
Nowack, W.J., Theodoridis, G.C., 1991. The thalamocortical contribution to epilepsy. Bull. Math. Biol. 53, 505–523. https://doi.org/10.1007/BF02458626.
O'Reilly, C., Iavarone, E., Hill, S.L., 2017. A framework for collaborative curation of neuroscientific literature. Front. Neuroinformatics 11. https://doi.org/10.3389/fninf.2017.00027.
O'Reilly, C., Iavarone, E., Jimenez, S., 2018. BlueBrain/corpus-thalamus. The Blue Brain Project.
Oh, S.W., Harris, J.A., Ng, L., Winslow, B., Cain, N., Mihalas, S., Wang, Q., Lau, C., Kuan, L., Henry, A.M., Mortrud, M.T., Ouellette, B., Nguyen, T.N., Sorensen, S.A., Slaughterbeck, C.R., Wakeman, W., Li, Y., Feng, D., Ho, A., Nicholas, E., Hirokawa, K.E., Bohn, P., Joines, K.M., Peng, H., Hawrylycz, M.J., Phillips, J.W., Hohmann, J.G., Wohnoutka, P., Gerfen, C.R., Koch, C., Bernard, A., Dang, C., Jones, A.R., Zeng, H., 2014. A mesoscale connectome of the mouse brain. Nature 508, 207–214. https://doi.org/10.1038/nature13186.
Ohara, P.T., Havton, L.A., 1996. Dendritic arbors of neurons from different regions of the rat thalamic reticular nucleus share a similar orientation. Brain Res. 731, 236–240.
Ohno, S., Kuramoto, E., Furuta, T., Hioki, H., Tanaka, Y.R., Fujiyama, F., Sonomura, T., Uemura, M., Sugiyama, K., Kaneko, T., 2012. A morphological analysis of thalamocortical axon fibers of rat posterior thalamic nuclei: a single neuron tracing study with viral vectors. Cereb. Cortex N. Y. N 1991 (22), 2840–2857. https://doi.org/10.1093/cercor/bhr356.
Okoyama, S., Moriizumi, T., 2001. Onset of calbindin-D 28K and parvalbumin expression in the lateral geniculate complex and olivary pretectal nucleus during postnatal development of the rat. Int. J. Dev. Neurosci. Off. J. Int. Soc. Dev. Neurosci. 19, 655–661.
Ottersen, O.P., Storm-Mathisen, J., 1984. GABA-containing neurons in the thalamus and pretectum of the rodent. An immunocytochemical study. Anat. Embryol. (Berl.) 170, 197–207.
Pape, H.C., Budde, T., Mager, R., Kisvárday, Z.F., 1994. Prevention of Ca(2+)-mediated action potentials in GABAergic local circuit neurones of rat thalamus by a transient K + current. J. Physiol. 478 (Pt 3), 403–422. https://doi.org/10.1113/jphysiol.1994.sp020261.
Papp, E.A., Leergaard, T.B., Calabrese, E., Johnson, G.A., Bjaalie, J.G., 2014. Waxholm space atlas of the Sprague Dawley rat brain. NeuroImage 97, 374–386. https://doi.org/10.1016/j.neuroimage.2014.04.001.
Parent, M., Descarries, L., 2008. Acetylcholine innervation of the adult rat thalamus: distribution and ultrastructural features in dorsolateral geniculate, parafascicular, and reticular thalamic nuclei. J. Comp. Neurol. 511, 678–691. https://doi.org/10.1002/cne.21868.
Parker, P.R.L., Cruikshank, S.J., Connors, B.W., 2009. Stability of electrical coupling despite massive developmental changes of intrinsic neuronal physiology. J. Neurosci. Off. J. Soc. Neurosci. 29, 9761–9770. https://doi.org/10.1523/JNEUROSCI.4568-08.2009.
Parri, H.R., Crunelli, V., 1998. Sodium current in rat and cat thalamocortical neurons: role of a non-inactivating component in tonic and burst firing. J. Neurosci. Off. J. Soc. Neurosci. 18, 854–867.
Parri, H.R., Gould, T.M., Crunelli, V., 2010. Sensory and cortical activation of distinct glial cell subtypes in the somatosensory thalamus of young rats. Eur. J. Neurosci. 32, 29–40. https://doi.org/10.1111/j.1460-9568.2010.07281.x.
Paxinos, G., Franklin, K.B.J., 2013. The mouse brain in stereotaxic coordinates. Mouse Brain in Stereotaxic Coordinates, 4th ed. Elsevier Academic Press, Amsterdam, Amsterdam.
Paxinos, G., Watson, C., 2014. The rat brain in stereotaxic coordinates. Paxinos and Watson's the Rat Brain in Stereotaxic Coordinates, 7th ed. Elsevier, Amsterdam, Amsterdam.
Penny, G.R., Fitzpatrick, D., Schmechel, D.E., Diamond, I.T., 1983. Glutamic acid decarboxylase-immunoreactive neurons and horseradish peroxidase-labeled

projection neurons in the ventral posterior nucleus of the cat and Galago senegalensis. J. Neurosci. Off. J. Soc. Neurosci. 3, 1868–1887.
Pierret, T., Lavallee, P., Deschenes, M., 2000. Parallel streams for the relay of vibrissal information through thalamic barreloids. J. Neurosci. Off. J. Soc. Neurosci. 20, 7455–7462.
Pinault, D., 2003. Cellular interactions in the rat somatosensory thalamocortical system during normal and epileptic 5-9 Hz oscillations. J. Physiol. 552, 881–905. https://doi.org/10.1113/jphysiol.2003.046573.
Pinault, D., 2004. The thalamic reticular nucleus: structure, function and concept. Brain Res. Brain Res. Rev. 46, 1–31. https://doi.org/10.1016/j.brainresrev.2004.04.008.
Pinault, D., Deschênes, M., 1998a. Projection and innervation patterns of individual thalamic reticular axons in the thalamus of the adult rat: a three-dimensional, graphic, and morphometric analysis. J. Comp. Neurol. 391, 180–203.
Pinault, D., Deschênes, M., 1998b. Anatomical evidence for a mechanism of lateral inhibition in the rat thalamus. Eur. J. Neurosci. 10, 3462–3469.
Pinault, D., Bourassa, J., Deschênes, M., 1995a. The axonal arborization of single thalamic reticular neurons in the somatosensory thalamus of the rat. Eur. J. Neurosci. 7, 31–40.
Pinault, D., Bourassa, J., Deschênes, M., 1995b. Thalamic reticular input to the rat visual thalamus: a single fiber study using biocytin as an anterograde tracer. Brain Res. 670, 147–152.
Piscopo, D.M., El-Danaf, R.N., Huberman, A.D., Niell, C.M., 2013. Diverse visual features encoded in mouse lateral geniculate nucleus. J. Neurosci. Off. J. Soc. Neurosci. 33, 4642–4656. https://doi.org/10.1523/JNEUROSCI.5187-12.2013.
Pita-Almenar, J.D., Yu, D., Lu, H.-C., Beierlein, M., 2014. Mechanisms underlying desynchronization of cholinergic-evoked thalamic network activity. J. Neurosci. Off. J. Soc. Neurosci. 34, 14463–14474. https://doi.org/10.1523/JNEUROSCI.2321-14.2014.
Power, B.D., Mitrofanis, J., 1999. Evidence for extensive inter-connections within the zona incerta in rats. Neurosci. Lett. 267, 9–12. https://doi.org/10.1016/s0304-3940(99)00313-4.
Prevosto, V., Sommer, M., 2013. Cognitive control of movement via the cerebellar-recipient thalamus. Front. Syst. Neurosci. 7 https://doi.org/10.3389/fnsys.2013.00056.
Puelles, L., Martinez-de-la-Torre, M., Bardet, S., Rubenstein, J.L.R., Puelles, L., 2012. Chapter 8 - Hypothalamus. In: Watson, C., Paxinos, G. (Eds.), The Mouse Nervous System. Academic Press, San Diego, pp. 221–312. https://doi.org/10.1016/B978-0-12-369497-3.10008-1.
Ralston, H.J., 1971. Evidence for presynaptic dendrites and a proposal for their mechanism of action. Nature 230, 585–587. https://doi.org/10.1038/230585a0.
Ramos, R., Requena, V., Diaz, F., Villena, A., Perez de Vargas, I., 1995. Evolution of neuronal density in the ageing thalamic reticular nucleus. Mech. Ageing Dev. 83, 21–29.
Rausell, E., Jones, E.G., 1991. Histochemical and immunocytochemical compartments of the thalamic VPM nucleus in monkeys and their relationship to the representational map. J. Neurosci. Off. J. Soc. Neurosci. 11, 210–225.
Rausell, E., Bae, C.S., Viñuela, A., Huntley, G.W., Jones, E.G., 1992. Calbindin and parvalbumin cells in monkey VPL thalamic nucleus: distribution, laminar cortical projections, and relations to spinothalamic terminations. J. Neurosci. Off. J. Soc. Neurosci. 12, 4088–4111.
Ray, A., Zoidl, G., Weickert, S., Wahle, P., Dermietzel, R., 2005. Site-specific and developmental expression of pannexin1 in the mouse nervous system. Eur. J. Neurosci. 21, 3277–3290. https://doi.org/10.1111/j.1460-9568.2005.04139.x.
Reardon, S., 2017. A giant neuron found wrapped around entire mouse brain. Nat. News 543, 14. https://doi.org/10.1038/nature.2017.21539.
Reese, B.E., 1988. 'Hidden lamination' in the dorsal lateral geniculate nucleus: the functional organization of this thalamic region in the rat. Brain Res. Rev. 13, 119–137. https://doi.org/10.1016/0165-0173(88)90017-3.
Reese, B.E., Jeffery, G., 1983. Crossed and uncrossed visual topography in dorsal lateral geniculate nucleus of the pigmented rat. J. Neurophysiol. 49, 877–885. https://doi.org/10.1152/jn.1983.49.4.877.
Reichova, I., Sherman, S.M., 2004. Somatosensory corticothalamic projections: distinguishing drivers from modulators. J. Neurophysiol. 92, 2185–2197. https://doi.org/10.1152/jn.00322.2004.
Reinhold, K., Lien, A.D., Scanziani, M., 2015. Distinct recurrent versus afferent dynamics in cortical visual processing. Nat. Neurosci. 18, 1789–1797. https://doi.org/10.1038/nn.4153.
Ross, D.T., Brasko, J., Patrikios, P., 1995. The AMPA antagonist NBQX protects thalamic reticular neurons from degeneration following cardiac arrest in rats. Brain Res. 683, 117–128.
Roth, M.M., Dahmen, J.C., Muir, D.R., Imhof, F., Martini, F.J., Hofer, S.B., 2016. Thalamic nuclei convey diverse contextual information to layer 1 of visual cortex. Nat. Neurosci. 19, 299–307. https://doi.org/10.1038/nn.4197.
Rouiller, E.M., Welker, E., 1991. Morphology of corticothalamic terminals arising from the auditory cortex of the rat: a Phaseolus vulgaris-leucoagglutinin (PHA-L) tracing study. Hear. Res. 56, 179–190. https://doi.org/10.1016/0378-5955(91)90168-9.
Rouiller, E.M., Welker, E., 2000. A comparative analysis of the morphology of corticothalamic projections in mammals. Brain Res. Bull. 53, 727–741. https://doi.org/10.1016/s0361-9230(00)00364-6.
Rouiller, E.M., Liang, F.Y., Moret, V., Wiesendanger, M., 1991. Patterns of corticothalamic terminations following injection of Phaseolus vulgaris leucoagglutinin (PHA-L) in the sensorimotor cortex of the rat. Neurosci. Lett. 125, 93–97. https://doi.org/10.1016/0304-3940(91)90139-k.
Rubio-Garrido, P., Pérez-de-Manzo, F., Clascá, F., 2007. Calcium-binding proteins as markers of layer-I projecting vs. deep layer-projecting thalamocortical neurons: a double-labeling analysis in the rat. Neuroscience 149, 242–250. https://doi.org/10.1016/j.neuroscience.2007.07.036.
Rubio-Garrido, P., Pérez-de-Manzo, F., Porrero, C., Galazo, M.J., Clascá, F., 2009. Thalamic input to distal apical dendrites in neocortical layer 1 is massive and highly convergent. Cereb. Cortex 19, 2380–2395. https://doi.org/10.1093/cercor/bhn259.
Saalmann, Y.B., Kastner, S., 2015. The cognitive thalamus. Front. Syst. Neurosci. 9 https://doi.org/10.3389/fnsys.2015.00039.
Santoro, B., Chen, S., Lüthi, A., Pavlidis, P., Shumyatsky, G.P., Tibbs, G.R., Siegelbaum, S. A., 2000. Molecular and functional heterogeneity of hyperpolarization-activated pacemaker channels in the mouse CNS. J. Neurosci. 20, 5264–5275. https://doi.org/10.1523/JNEUROSCI.20-14-05264.2000.
Sanz Leon, P., Knock, S.A., Woodman, M.M., Domide, L., Mersmann, J., McIntosh, A.R., Jirsa, V., 2013. The Virtual Brain: a simulator of primate brain network dynamics. Front. Neuroinformatics 7. https://doi.org/10.3389/fninf.2013.00010.
Saporta, S., Kruger, L., 1977. The organization of thalamocortical relay neurons in the rat ventrobasal complex studied by the retrograde transport of horseradish peroxidase. J. Comp. Neurol. 174, 187–208. https://doi.org/10.1002/cne.901740202.
Sausbier, U., Sausbier, M., Sailer, C.A., Arntz, C., Knaus, H.-G., Neuhuber, W., Ruth, P., 2006. Ca2+ -activated K+ channels of the BK-type in the mouse brain. Histochem. Cell Biol. 125, 725–741. https://doi.org/10.1007/s00418-005-0124-7.
Sawyer, S.F., Tepper, J.M., Groves, P.M., 1994. Cerebellar-responsive neurons in the thalamic ventroanterior-ventrolateral complex of rats: light and electron microscopy. Neuroscience 63, 725–745.
Schmitt, L.I., Wimmer, R.D., Nakajima, M., Happ, M., Mofakham, S., Halassa, M.M., 2017. Thalamic amplification of cortical connectivity sustains attentional control. Nature 545, 219–223. https://doi.org/10.1038/nature22073.
Schulman, J.J., Cancro, R., Lowe, S., Lu, F., Walton, K.D., Llinás, R.R., 2011. Imaging of thalamocortical dysrhythmia in neuropsychiatry. Front. Hum. Neurosci. 5 https://doi.org/10.3389/fnhum.2011.00069.
Schumann, T., Erő, C., Gewaltig, M.-O., Delalondre, F.J., 2017. Towards simulating data-driven brain models at the point neuron level on petascale computers. In: Di Napoli, E., Hermanns, M.-A., Iliev, H., Lintermann, A., Peyser, A. (Eds.), High-Performance Scientific Computing, Lecture Notes in Computer Science. Springer International Publishing, pp. 160–169.
Sevetson, J., Haas, J.S., 2015. Asymmetry and modulation of spike timing in electrically coupled neurons. J. Neurophysiol. 113, 1743–1751. https://doi.org/10.1152/jn.00843.2014.
Sevetson, J., Fittro, S., Heckman, E., Haas, J.S., 2017. A calcium-dependent pathway underlies activity-dependent plasticity of electrical synapses in the thalamic reticular nucleus. J. Physiol. 595, 4417–4430. https://doi.org/10.1113/JP274049.
Sherman, S.M., 2001. Tonic and burst firing: dual modes of thalamocortical relay. Trends Neurosci. 24, 122–126. https://doi.org/10.1016/S0166-2236(00)01714-8.
Sherman, S.M., 2004. Interneurons and triadic circuitry of the thalamus. Trends Neurosci. 27, 670–675. https://doi.org/10.1016/j.tins.2004.08.003.
Sherman, S.M., Guillery, R.W., 1996. Functional organization of thalamocortical relays. J. Neurophysiol. 76, 1367–1395.
Sherman, S.M., Koch, C., 1986. The control of retinogeniculate transmission in the mammalian lateral geniculate nucleus. Exp. Brain Res. 63, 1–20. https://doi.org/10.1007/BF00235642.
Shosaku, A., 1986. Cross-correlation analysis of a recurrent inhibitory circuit in the rat thalamus. J. Neurophysiol. 55, 1030–1043.
Shosaku, A., Kayama, Y., Sumitomo, I., 1984. Somatotopic organization in the rat thalamic reticular nucleus. Brain Res. 311, 57–63.
Sieg, F., Obst, K., Gorba, T., Riederer, B., Pape, H.C., Wahle, P., 1998. Postnatal expression pattern of calcium-binding proteins in organotypic thalamic cultures and in the dorsal thalamus in vivo. Brain Res. Dev. Brain Res. 110, 83–95.
Skåtun, K.C., Kaufmann, T., Brandt, C.L., Doan, N.T., Alnæs, D., Tønnesen, S., Biele, G., Vaskinn, A., Melle, I., Agartz, I., Andreassen, O.A., Westlye, L.T., 2018. Thalamo-cortical functional connectivity in schizophrenia and bipolar disorder. Brain Imaging Behav. 12, 640–652. https://doi.org/10.1007/s11682-017-9714-y.
Smith, G.D., Cox, C.L., Sherman, S.M., Rinzel, J., 2001. A firing-rate model of spike-frequency adaptation in sinusoidally-driven thalamocortical relay neurons. Thalamus Relat. Syst. 1, 135–156. https://doi.org/10.1016/S1472-9288(01)00012-7.
Soltesz, I., Crunelli, V., 1992. A role for low-frequency, rhythmic synaptic potentials in the synchronization of cat thalamocortical cells. J. Physiol. 457, 257–276. https://doi.org/10.1113/jphysiol.1992.sp019377.
Spacek, J., Lieberman, A.R., 1974. Ultrastructure and three-dimensional organization of synaptic glomeruli in rat somatosensory thalamus. J. Anat. 117, 487–516.
Spreafico, R., Schmechel, D.E., Ellis, L.C., Rustioni, A., 1983. Cortical relay neurons and interneurons in the N. Ventralis posterolateralis of cats: a horseradish peroxidase, electron-microscopic, Golgi and immunocytochemical study. Neuroscience 9, 491–509. https://doi.org/10.1016/0306-4522(83)90168-9.
Spreafico, R., Barbaresi, P., Weinberg, R.J., Rustioni, A., 1987. SII-projecting neurons in the rat thalamus: a single- and double-retrograde-tracing study. Somatosens. Res. 4, 359–375.
Spreafico, R., de Curtis, M., Frassoni, C., Avanzini, G., 1988. Electrophysiological characteristics of morphologically identified reticular thalamic neurons from rat slices. Neuroscience 27, 629–638.
Spreafico, R., Battaglia, G., Frassoni, C., 1991. The reticular thalamic nucleus (RTN) of the rat: cytoarchitectural, Golgi, immunocytochemical, and horseradish peroxidase study. J. Comp. Neurol. 304, 478–490. https://doi.org/10.1002/cne.903040311.
Stehberg, J., Acuna-Goycolea, C., Ceric, F., Torrealba, F., 2001. The visceral sector of the thalamic reticular nucleus in the rat. Neuroscience 106, 745–755.
Steriade, M., 2000. Corticothalamic resonance, states of vigilance and mentation. Neuroscience 101, 243–276. https://doi.org/10.1016/s0306-4522(00)00353-5.

Steriade, M., 2006. Grouping of brain rhythms in corticothalamic systems. Neuroscience 137, 1087–1106. https://doi.org/10.1016/j.neuroscience.2005.10.029.
Steriade, M., Deschênes, M., Domich, L., Mulle, C., 1985. Abolition of spindle oscillations in thalamic neurons disconnected from nucleus reticularis thalami. J. Neurophysiol. 54, 1473–1497. https://doi.org/10.1152/jn.1985.54.6.1473.
Steriade, M., Domich, L., Oakson, G., Deschênes, M., 1987. The deafferented reticular thalamic nucleus generates spindle rhythmicity. J. Neurophysiol. 57, 260–273. https://doi.org/10.1152/jn.1987.57.1.260.
Steriade, M., Dossi, R.C., Nuñez, A., 1991. Network modulation of a slow intrinsic oscillation of cat thalamocortical neurons implicated in sleep delta waves: cortically induced synchronization and brainstem cholinergic suppression. J. Neurosci. Off. J. Soc. Neurosci. 11, 3200–3217.
Steriade, M., Contreras, D., Curró Dossi, R., Nuñez, A., 1993. The slow (< 1 Hz) oscillation in reticular thalamic and thalamocortical neurons: scenario of sleep rhythm generation in interacting thalamic and neocortical networks. J. Neurosci. Off. J. Soc. Neurosci. 13, 3284–3299.
Sugitani, M., Yano, J., Sugai, T., Ooyama, H., 1990. Somatotopic organization and columnar structure of vibrissae representation in the rat ventrobasal complex. Exp. Brain Res. 81, 346–352. https://doi.org/10.1007/BF00228125.
Sumser, A., Mease, R.A., Sakmann, B., Groh, A., 2017. Organization and somatotopy of corticothalamic projections from L5B in mouse barrel cortex. Proc. Natl. Acad. Sci. U. S. A. 114, 8853–8858. https://doi.org/10.1073/pnas.1704302114.
Sun, Q.-Q., Huguenard, J.R., Prince, D.A., 2002. Somatostatin inhibits thalamic network oscillations in vitro: actions on the GABAergic neurons of the reticular nucleus. J. Neurosci. Off. J. Soc. Neurosci. 22, 5374–5386 https://doi.org/20026529.
Sun, Q.-Q., Baraban, S.C., Prince, D.A., Huguenard, J.R., 2003. Target-specific neuropeptide Y-ergic synaptic inhibition and its network consequences within the mammalian thalamus. J. Neurosci. Off. J. Soc. Neurosci. 23, 9639–9649.
Talley, E.M., Cribbs, L.L., Lee, J.H., Daud, A., Perez-Reyes, E., Bayliss, D.A., 1999. Differential distribution of three members of a gene family encoding low voltage-activated (T-type) calcium channels. J. Neurosci. Off. J. Soc. Neurosci. 19, 1895–1911.
Timofeev, I., Bazhenov, M., Seigneur, J., Sejnowski, T., 2012. Neuronal synchronization and thalamocortical rhythms in sleep, wake and epilepsy. In: Noebels, J.L., Avoli, M., Rogawski, M.A., Olsen, R.W., Delgado-Escueta, A.V. (Eds.), Jasper's Basic Mechanisms of the Epilepsies. National Center for Biotechnology Information (US), Bethesda (MD).
Tsukano, H., Horie, M., Ohga, S., Takahashi, K., Kubota, Y., Hishida, R., Takebayashi, H., Shibuki, K., 2017. Reconsidering tonotopic maps in the auditory cortex and lemniscal auditory thalamus in mice. Front. Neural Circuits 11. https://doi.org/10.3389/fncir.2017.00014.
Turner, J.P., Anderson, C.M., Williams, S.R., Crunelli, V., 1997. Morphology and membrane properties of neurones in the cat ventrobasal thalamus in vitro. J. Physiol. 505, 707–726.
Van Der Loos, H., 1976. Barreloids in mouse somatosensory thalamus. Neurosci. Lett. 2, 1–6. https://doi.org/10.1016/0304-3940(76)90036-7.
Vantomme, G., Osorio-Forero, A., Lüthi, A., Fernandez, L.M.J., 2019. Regulation of local sleep by the thalamic reticular nucleus. Front. Neurosci. 13 https://doi.org/10.3389/fnins.2019.00576.
Veinante, P., Jacquin, M.F., Deschênes, M., 2000. Thalamic projections from the whisker-sensitive regions of the spinal trigeminal complex in the rat. J. Comp. Neurol. 420, 233–243.
Vigeland, L.E., Contreras, D., Palmer, L.A., 2013. Synaptic mechanisms of temporal diversity in the lateral geniculate nucleus of the thalamus. J. Neurosci. 33, 1887–1896. https://doi.org/10.1523/JNEUROSCI.4046-12.2013.
Waite, P.M., 1973. Somatotopic organization of vibrissal responses in the ventro-basal complex of the rat thalamus. J. Physiol. 228, 527–540. https://doi.org/10.1113/jphysiol.1973.sp010098.
Wanaverbecq, N., Bodor, A.L., Bokor, H., Slezia, A., Luthi, A., Acsady, L., 2008. Contrasting the functional properties of GABAergic axon terminals with single and multiple synapses in the thalamus. J. Neurosci. Off. J. Soc. Neurosci. 28, 11848–11861. https://doi.org/10.1523/JNEUROSCI.3183-08.2008.
Werner, L., Neumann, E., Winkelmann, E., 1984. [Morphometric analysis of the dorsal lateral geniculate body of the laboratory mouse and microphthalmic variants]. Z. Mikrosk. Anat. Forsch. 98, 119–136.
Weyand, T.G., Boudreaux, M., Guido, W., 2001. Burst and Tonic Response Modes in Thalamic Neurons During Sleep and Wakefulness. J. Neurophysiol. 85, 1107–1118. https://doi.org/10.1152/jn.2001.85.3.1107.
Whitmire, C.J., Millard, D.C., Stanley, G.B., 2017. Thalamic state control of cortical paired-pulse dynamics. J. Neurophysiol. 117, 163–177. https://doi.org/10.1152/jn.00415.2016.
Williams, S.R., Stuart, G.J., 2000. Action potential backpropagation and somato-dendritic distribution of ion channels in thalamocortical neurons. J. Neurosci. Off. J. Soc. Neurosci. 20, 1307–1317.
Williams, M.N., Zahm, D.S., Jacquin, M.F., 1994. Differential foci and synaptic organization of the principal and spinal trigeminal projections to the thalamus in the rat. Eur. J. Neurosci. 6, 429–453. https://doi.org/10.1111/j.1460-9568.1994.tb00286.x.
Williams, S.R., Turner, J.P., Anderson, C.M., Crunelli, V., 1996. Electrophysiological and morphological properties of interneurones in the rat dorsal lateral geniculate nucleus in vitro. J. Physiol. 490, 129–147.
Wimmer, R.D., Astori, S., Bond, C.T., Rovó, Z., Chatton, J.-Y., Adelman, J.P., Franken, P., Lüthi, A., 2012. Sustaining sleep spindles through enhanced SK2-channel activity consolidates sleep and elevates arousal threshold. J. Neurosci. Off. J. Soc. Neurosci. 32, 13917–13928. https://doi.org/10.1523/JNEUROSCI.2313-12.2012.
Wimmer, R.D., Schmitt, L.I., Davidson, T.J., Nakajima, M., Deisseroth, K., Halassa, M.M., 2015. Thalamic control of sensory selection in divided attention. Nature 526, 705–709. https://doi.org/10.1038/nature15398.
Winnubst, J., Bas, E., Ferreira, T.A., Wu, Z., Economo, M.N., Edson, P., Arthur, B.J., Bruns, C., Rokicki, K., Schauder, D., Olbris, D.J., Murphy, S.D., Ackerman, D.G., Arshadi, C., Baldwin, P., Blake, R., Elsayed, A., Hasan, M., Ramirez, D., Dos Santos, B., Weldon, M., Zafar, A., Dudman, J.T., Gerfen, C.R., Hantman, A.W., Korff, W., Sternson, S.M., Spruston, N., Svoboda, K., Chandrashekar, J., 2019. Reconstruction of 1,000 projection neurons reveals new cell types and organization of long-range connectivity in the mouse brain. Cell 179, 268–281. https://doi.org/10.1016/j.cell.2019.07.042 e13.
Winsky, L., Montpied, P., Arai, R., Martin, B.M., Jacobowitz, D.M., 1992. Calretinin distribution in the thalamus of the rat: immunohistochemical and in situ hybridization histochemical analyses. Neuroscience 50, 181–196. https://doi.org/10.1016/0306-4522(92)90391-e.
Wolff, M., Vann, S.D., 2019. The cognitive thalamus as a gateway to mental representations. J. Neurosci. 39, 3–14. https://doi.org/10.1523/JNEUROSCI.0479-18.2018.
Woodward, N.D., Karbasforoushan, H., Heckers, S., 2012. Thalamocortical dysconnectivity in schizophrenia. Am. J. Psychiatry 169, 1092–1099. https://doi.org/10.1176/appi.ajp.2012.12010056.
Woodward, N.D., Giraldo-Chica, M., Rogers, B., Cascio, C.J., 2017. Thalamocortical dysconnectivity in autism spectrum disorder: an analysis of the autism brain imaging data exchange. Biol. Psychiatry Cogn. Neurosci. Neuroimaging 2, 76–84. https://doi.org/10.1016/j.bpsc.2016.09.002.
Yamada, A., Saji, M., Ukita, Y., Shinoda, Y., Taniguchi, M., Higaki, K., Ninomiya, H., Ohno, K., 2001. Progressive neuronal loss in the ventral posterior lateral and medial nuclei of thalamus in Niemann-Pick disease type C mouse brain. Brain Dev. 23, 288–297. https://doi.org/10.1016/s0387-7604(01)00209-1.
Yang, Sunggu, Govindaiah, G., Lee, S.-H., Yang, Sungchil, Cox, C.L., 2017. Distinct kinetics of inhibitory currents in thalamocortical neurons that arise from dendritic or axonal origin. PLoS One 12, e0189690. https://doi.org/10.1371/journal.pone.0189690.
Yu, C., Derdikman, D., Haidarliu, S., Ahissar, E., 2006. Parallel thalamic pathways for whisking and touch signals in the rat. PLoS Biol. 4, e124. https://doi.org/10.1371/journal.pbio.0040124.
Zappala, A., Cicero, D., Serapide, M.F., Paz, C., Catania, M.V., Falchi, M., Parenti, R., Panto, M.R., La Delia, F., Cicirata, F., 2006. Expression of pannexin1 in the CNS of adult mouse: cellular localization and effect of 4-aminopyridine-induced seizures. Neuroscience 141, 167–178. https://doi.org/10.1016/j.neuroscience.2006.03.053.
Zhang, Y., Mori, M., Burgess, D.L., Noebels, J.L., 2002. Mutations in high-voltage-activated calcium channel genes stimulate low-voltage-Activated currents in mouse thalamic relay neurons. J. Neurosci. 22, 6362–6371. https://doi.org/10.1523/JNEUROSCI.22-15-06362.2002.
Zhang, L., Liang, B., Barbera, G., Hawes, S., Zhang, Y., Stump, K., Baum, I., Yang, Y., Li, Y., Lin, D.-T., 2019. Miniscope GRIN lens system for calcium imaging of neuronal activity from deep brain structures in behaving animals. Curr. Protoc. Neurosci. 86, e56. https://doi.org/10.1002/cpns.56.
Zhu, J.J., Lo, F.S., 1999a. Three GABA receptor-mediated postsynaptic potentials in interneurons in the rat lateral geniculate nucleus. J. Neurosci. Off. J. Soc. Neurosci. 19, 5721–5730.
Zhu, J.J., Lo, F.S., 1999b. Three GABA receptor-mediated postsynaptic potentials in interneurons in the rat lateral geniculate nucleus. J. Neurosci. Off. J. Soc. Neurosci. 19, 5721–5730.
Zobeiri, M., Chaudhary, R., Blaich, A., Rottmann, M., Herrmann, S., Meuth, P., Bista, P., Kanyshkova, T., Lüttjohann, A., Narayanan, V., Hundehege, P., Meuth, S.G., Romanelli, M.N., Urbano, F.J., Pape, H.-C., Budde, T., Ludwig, A., 2019. The hyperpolarization-activated HCN4 channel is important for proper maintenance of oscillatory activity in the thalamocortical system. Cereb. Cortex N. Y. NY 29, 2291–2304. https://doi.org/10.1093/cercor/bhz047.
Zolnik, T.A., Connors, B.W., 2016. Electrical synapses and the development of inhibitory circuits in the thalamus. J. Physiol. 594, 2579–2592. https://doi.org/10.1113/JP271880.